NATIONAL ADVISORY COMMITTEE FOR AERONAUTICS

TECHNICAL NOTE 2656

A BLADE-ELEMENT ANALYSIS FOR LIFTING ROTORS THAT IS APPLICABLE FOR LARGE INFLOW AND BLADE ANGLES AND ANY REASONABLE BLADE GEOMETRY

By Walter Castles, Jr., and Noah C. New

Georgia Institute of Technology

NACA

Washington

July 1952

NATIONAL ADVISORY COMMITTEE FOR AERONAUTICS

TECHNICAL NOTE 2656

A BLADE-ELEMENT ANALYSIS FOR LIFTING ROTORS THAT IS APPLICABLE FOR LARGE INFLOW AND BLADE ANGLES AND ANY REASONABLE BLADE GEOMETRY

By Walter Castles, Jr., and Noah C. New

SUMMARY

Simple approximate solutions are derived for the relationships between the rotor thrust and flight-path velocity components and the rotor blade angle, torque, and in-plane forces. These approximate solutions, based upon the assumption of a triangular distribution of blade circulation and a parabolic variation of blade-element profile drag with lift, are sufficiently accurate for preliminary calculations and the determination of the equilibrium angle of attack and lateral tilt of the tip-path plane.

A set of more exact blade-element equations is then derived giving the relations between the thrust and flight-path velocity components and the equilibrium blade angles, torque, and in-plane forces and moments. Neither the blade-element nor the approximate solutions are dependent upon the usual approximations that the inflow angle and blade angle of the blade elements are small angles. Thus the present equations should be useful for convertaplane as well as helicopter calculations.

It appears that nonlinear blade twist may be desirable for a convertaplane rotor in order to obtain useful propeller efficiencies. Therefore, the blade-element equations have been arranged so that any reasonable distribution of blade twist may be used. Also, the equations were set up in terms of an arbitrary blade-chord distribution since it was found that the use of the actual blade-chord distribution and the elimination of the usual assumption that the blade airfoil extended inboard to the axis of rotation largely eliminated the necessity for the usual reverse-flow corrections. Tables of the necessary factors are included for blades having a linear taper, linear twist, and an airfoil contour from $r = 0.15R$ to $r = R$ and for blades having a linear taper, helical twist, and airfoil contours extending from $r = 0.20R$ to $r = R$ (where r is the radius of the blade element and R, the radius of the blade tip).

The present analysis is based upon the following assumptions:

(1) The blade-element lift coefficient may be assumed to be proportional to the sine of the blade-element angle of attack, and the blade-element profile-drag coefficient may be represented by the first three terms of a Fourier series in the blade-element angle of attack. This implies the neglect of blade stall effects in the equations for the blade angles. The effect of tip stall is taken into account in the equations for the rotor torque.

(2) The blade axes may be assumed to be, and to remain, straight lines.

(3) The lateral and longitudinal variations of the normal component of the induced velocity at the tip-path plane may be assumed to be linear.

(4) The effects of compressibility on the tip sections of the advancing blade may be neglected.

(5) All radial velocity components and the tangential components of the induced velocity may be neglected.

(6) Blade tip effects may be neglected.

A comparison of the results given by the present equations with the full-scale helicopter test data of NACA TN 1266 shows good agreement for the helicopter flight range covered in that report.

INTRODUCTION

This project, which was conducted at the Georgia Institute of Technology Engineering Experiment Station under the sponsorship and with the financial assistance of the National Advisory Committee for Aeronautics, was undertaken in order to develop a blade-element analysis for lifting rotors that would be useful for convertaplane calculations. This necessitated the elimination of the usual approximations that the blade-element inflow angle ϕ and the blade angle θ are small angles and required a reasonably exact treatment of the blade geometry.

It was found that a practical approach to the problem of eliminating the small-angle approximations for the lift forces could be obtained by writing the lift coefficient of the blade element as

$$c_l = a \sin \alpha_r = a\left(\sin \theta_v \cos \phi_v + \cos \theta_v \sin \phi_v\right)$$

and, consequently, the thrust component of force $dL \cos \phi_v$ on a blade element as

$$dL \cos \phi_v = \frac{1}{2} \rho a (U \cos \phi_v) \left[\sin \theta_v (U \cos \phi_v) + \cos \theta_v (U \sin \phi_v) \right] c \, dr$$

Similarly, the tangential component of the lift on a blade element may be expressed as

$$dL \sin \phi_v = \frac{1}{2} \rho a (U \sin \phi_v) \left[\sin \theta_v (U \cos \phi_v) + \cos \theta_v (U \sin \phi_v) \right] c \, dr$$

It was also found that the small-angle approximations could be largely eliminated for the profile-drag terms by expressing the blade-element profile-drag coefficient c_{d_o} as

$$c_{d_o} = \epsilon_0 + \epsilon_1 \sin \alpha_r + \epsilon_2 \cos \alpha_r$$

The exact blade geometry has been retained throughout by expressing the blade-chord and blade-twist distribution in the form of the following constants:

$$\sigma_n = \frac{1}{\pi R} \int_{x_1}^{1} c x^{n-1} \, dx$$

$$\sigma_{nc} = \frac{1}{\pi R} \int_{x_1}^{1} c \cos \theta_t x^{n-1} \, dx$$

and

$$\sigma_{ns} = \frac{1}{\pi R} \int_{x_1}^{1} c \sin \theta_t x^{n-1} \, dx$$

where θ_t is the blade twist in the angle of zero lift between the reference station and nondimensional radius x. Values of these constants are given in tables 1 to 3 for blades having linear taper, linear twist, and $x_1 = 0.15$ and in tables 1, 4, and 5 for blades having linear taper, helical twist, and $x_1 = 0.20$.

The present system of equations has been set up with respect to tip-path-plane coordinates or coordinates based on the virtual axis of rotation (fig. 1) rather than the usual coordinate system based on the plane of zero feathering in order to obtain shorter expressions for the in-plane rotor forces and moments. The use of coordinates alined with the virtual axis of rotation also facilitates the treatment of some accelerated flight problems.

Certain refinements in the induced-velocity theory, as given in reference 1, have been incorporated with some minor changes in the present equations along with the necessary terms for an arbitrary angular velocity of roll and pitch of the tip-path plane.

Standard NACA nomenclature has been used where possible, with the subscript v for virtual axis of rotation appended to the usual symbols which, in this paper, have a similar meaning but different numerical values.

NOTATION

a slope of lift curve for blade element at 0.75R (per radian)

a_0 rotor coning angle

$\bar{a}_0$ coning angle for zero blade-root bending moment

a_1 coefficient of sine component of blade cyclic-pitch angle measured with respect to tip-path plane where

$$\theta_v = A_0 + \theta_t - a_1 \sin \psi + b_1 \cos \psi$$

also coefficient of cosine term of Fourier series for blade flapping angle β measured with respect to plane of zero feathering where

$$\beta = a_0 - a_1 \cos \psi - b_1 \sin \psi - a_2 \cos 2\psi - b_2 \sin 2\psi - \ldots$$

a_2 coefficient of second-harmonic cosine term in Fourier series for blade flapping angle

A_0 mean blade pitch angle at reference station, positive above tip-path plane

b number of blades in rotor

b_1 coefficient of cosine component of blade cyclic-pitch angle measured with respect to the tip-path plane; also coefficient of sine term of Fourier series for blade flapping angle measured with respect to plane of zero feathering

b_2 coefficient of second-harmonic sine term in Fourier series for blade flapping angle

c blade chord at radius r

c_o extended blade-root chord at $r = 0$ (for linear taper)

c_{d_o} section profile-drag coefficient

c_l section lift coefficient

C_{mx} rotor rolling-moment coefficient measured about X-axis $\left(\frac{M_x}{\frac{1}{2}\rho\pi\Omega^2R^5}\right)$

C_{my} rotor pitching-moment coefficient measured about Y-axis $\left(\frac{M_y}{\frac{1}{2}\rho\pi\Omega^2R^5}\right)$

C_Q rotor torque coefficient $\left(\frac{Q}{\rho\pi\Omega^2R^5}\right)$

ΔC_{Q_s} increment to C_Q from tip stall on retreating blade

C_T rotor thrust coefficient $\left(\frac{T}{\rho\pi\Omega^2R^4}\right)$

C_x rotor X-force coefficient $\left(\frac{F_x}{\frac{1}{2}\rho\pi\Omega^2R^4}\right)$

C_{xy} rotor-blade tangential-force coefficient, positive in direction of rotation $\left(\frac{F_{xy}}{\frac{1}{2}\rho\pi\Omega^2R^4}\right)$

C_y rotor Y-force coefficient $\left(\frac{F_y}{\frac{1}{2}\rho\pi\Omega^2R^4}\right)$

C_z rotor-blade thrust-force coefficient $\left(\frac{F_z}{\frac{1}{2}\rho\pi\Omega^2R^4}\right)$

D_F fuselage and wing drag

D_o blade profile drag

E_0 mean blade drag angle, positive in direction of rotation and measured between blade axis and line through rotor axis of rotation and drag hinge (i.e., blade drag angle ζ is $\zeta = E_0 + E_1 \cos \psi + F_1 \sin \psi + \ldots$)

E_1 coefficient of cosine term in expression for blade drag angle

F_1 coefficient of sine term in expression for blade drag angle

F_x component of rotor resultant force acting along X-axis

F_{xy} tangential component of the resultant air force on blade, positive in direction of rotation

F_y component of rotor resultant force acting along Y-axis

F_z Z component of resultant air force on blade

g acceleration due to gravity

I_1 mass moment of inertia of blade about flapping hinge

$I_{nc} = \sigma_{nc} \sin A_0 + \sigma_{ns} \cos A_0$

$I_{ns} = \sigma_{ns} \sin A_0 - \sigma_{nc} \cos A_0$

I_v mass moment of inertia of rotor about virtual axis of rotation

I_ζ mass moment of inertia of blade about drag hinge

k_{a_0} blade-root spring constant (blade-root bending moment in foot-pounds divided by angular deflection in radians of three-quarter-radius point from $\overline{a}_0$)

L_F fuselage and wing lift

M_x rotor rolling moment

M_y rotor pitching moment

Q rotor torque, negative in direction of rotation

r radius of blade element $c\,dr$

$\overline{r}$ radius of blade center of gravity

r_1 radius of inboard blade airfoil element

r_β radius of flapping hinge

R radius of blade tip

$t = \frac{\text{Tip chord}}{c_0} - 1$ (for linearly tapered blades)

T rotor thrust, component of rotor resultant force along Z-axis

U component of resultant velocity at blade element that is normal to blade axis

v mean normal component of induced velocity at tip-path plane (positive down and to rear)

V velocity along flight path

V_i Z component of induced velocity at radius r and azimuth angle ψ (positive in plus Z-direction)

w slope of longitudinal variation of nondimensional induced velocity

W gross weight plus down component of any acceleration force acting on aircraft

x nondimensional blade radius (r/R)

x_s nondimensional radius outboard of which retreating blade is stalled

x_1 nondimensional radius of inboard blade airfoil element

y slope of lateral variation of nondimensional induced velocity

α_f angle of attack of fuselage measured between flight-path velocity vector and longitudinal fuselage axis

α_r blade-element angle of attack measured from line of zero lift

α_v angle of attack of tip-path plane measured in the XZ-plane between flight-path velocity vector and tip-path plane, positive below tip-path plane

β blade flapping angle at azimuth angle ψ (for tip-path plane,

$$\beta_v = a_0 - a_2 \cos 2\psi - b_2 \sin 2\psi - \ldots;$$

for plane of zero feathering,

$$\beta = a_0 - a_1 \cos \psi - b_1 \sin \psi - a_2 \cos 2\psi - b_2 \sin 2\psi - \ldots)$$

Γ circulation of blade element at radius r and azimuth angle ψ

Γ_0, Γ_1 constants in expression for Γ where $\Gamma = (\Gamma_0 + \Gamma_1 \sin \psi)x$

δ_0 value of c_{d_o} at $c_l = 0$

ϵ constant in power equation for c_{d_o} ($i.e.$, $c_{d_o} = \delta_0 + \epsilon c_l^2$)

$\epsilon_0, \epsilon_1, \epsilon_2$ constants for first three terms of Fourier series expressing relation between c_{d_o} and α_r ($i.e.$, $c_{d_o} = \epsilon_0 + \epsilon_1 \sin \alpha_r + \epsilon_2 \cos \alpha_r$ or $c_{d_o} = \epsilon_1 \sin \alpha_r + \epsilon_2 \cos \alpha_r$)

ζ blade drag angle at azimuth angle ψ, positive in direction of rotation

θ_l twist in zero-lift chord line between axis of rotation and blade tip for blades with linear twist, positive for increased angle at tip $\left(\text{i.e., } \theta_t = \theta_l x\right)$

θ_t twist in rotor blade angle of zero lift between reference station and radius r, positive for larger angle outboard

θ_T design helix angle at tip of blade for blades with helical twist

θ_v pitch angle of blade element at radius r and azimuth angle ψ measured between zero-lift chord line and tip-path plane, positive above tip-path plane $\left(A_0 + \theta_t - a_1 \sin \psi + b_1 \cos \psi\right)$

θ_x angular displacement of tip-path plane about X-axis from horizontal

θ_y angular displacement of tip-path plane about Y-axis from horizontal

λ_v inflow velocity ratio at center of tip-path plane $\left(\frac{V \sin \alpha_v - v}{\Omega R}\right)$

μ_v in-plane velocity ratio at tip-path plane $\left(\frac{V \cos \alpha_v}{\Omega R}\right)$

ρ density of air

$\sigma_n = \frac{1}{\pi R}\int_{x_l}^{1} cx^{n-l}\,dx$ constants which express blade-chord distribution $\left(\text{i.e., } \sigma_l = \frac{1}{\pi R}\int_{x_l}^{1} c\,dx\right.$

$\left.\sigma_2 = \frac{1}{\pi R}\int_{x_l}^{1} cx\,dx, \text{ etc.}\right)$

$$\sigma_{nc} = \frac{1}{\pi R}\int_{x_1}^{1} c \cos \theta_t x^{n-1}\, dx$$

$$\sigma_{ns} = \frac{1}{\pi R}\int_{x_1}^{1} c \sin \theta_t x^{n-1}\, dx$$

} constants which express blade-chord and blade-twist distribution

ϕ_c angle between flight path and horizontal, positive below horizontal

ϕ_v inflow angle at blade element measured in plane perpendicular to blade axis and between tip-path plane and relative wind, positive below tip-path plane

ψ azimuth angle of blade axis measured about Z-axis from X-axis (This angle is very nearly but not identically equal to the equivalent angle in plane of zero feathering.)

ω_x ratio of angular velocity of roll of tip-path plane about X-axis to Ω

ω_y ratio of angular velocity of pitch of tip-path plane about Y-axis to Ω

Ω mean angular velocity of rotor blade axis about Z-axis

All angles are in radian measure.

ANALYSIS

Value of Normal Component of Induced Velocity at Radius r and Azimuth Angle ψ

It is shown in reference 1 that for a lightly loaded single rotor composed of a large number of blades b each having a circulation given by the expression

$$\Gamma = \Gamma_0 + \Gamma_1 \sin \psi \qquad (1)$$

the mean value of the normal component of the induced velocity is

$$v = \frac{\frac{1}{2}\Omega R C_T}{\left(1 - \frac{3}{2}\mu_v^2\right)\sqrt{\lambda_v^2 + \mu_v^2}} \tag{2}$$

Equation (2) was derived on the assumption that the wake extended to infinity and had the form of a straight elliptic cylinder. Thus, for those flight conditions where a "vortex ring" type flow exists, equation (2) is not applicable and the value of v must, at present, be obtained from experiment. The term $\left(1 - \frac{3}{2}\mu_v^2\right)$ in the denominator of equation (2) arises from the lateral dissymmetry in the blade circulation that is required for rolling-moment equilibrium, and this term is the only correction which the elementary theory makes in Glauert's original hypothesis that $v = T/2\rho AV'$, where V' is the resultant velocity at the center of the rotor.

If the distribution of the normal component of the induced velocity V_i over the tip-path plane is denoted by a power series in the nondimensional radius x and a Fourier series in the azimuth angle ψ such that for the first-order terms

$$\frac{V_i}{\Omega R} = -\frac{v}{\Omega R} + wx \cos\psi + yx \sin\psi \tag{3}$$

it can be shown from the results of reference 1 that

$$w \approx -\frac{4}{3}\left[\left(1 - 1.8\mu_v^2\right)\sqrt{1 + \left(\frac{\lambda_v}{\mu_v}\right)^2} - \sqrt{\left(\frac{\lambda_v}{\mu_v}\right)^2}\right]\frac{v}{\Omega R} \tag{4}$$

and

$$y \approx 2\mu_v \frac{v}{\Omega R} \tag{5}$$

For level flight and $\mu_v > 0.15$ the expression for y may be simplified to

$$y \approx C_T \tag{6}$$

It may be noted that for a pair of equally loaded, coaxial, counter-rotating rotors, the values of w and y are

$$w \approx -\frac{4}{3}\left[\sqrt{1 + \left(\frac{\lambda_v}{\mu_v}\right)^2} - \sqrt{\left(\frac{\lambda_v}{\mu_v}\right)^2}\right]\frac{v}{\Omega R} \tag{7}$$

and

$$y = 0 \tag{8}$$

Approximate Values of Rotor Blade Angles, Torque, and X-Force and Y-Force Coefficients

It is convenient for preliminary calculations and checking and necessary, in the general case, for the determination of the angle of attack and lateral tilt of the tip-path plane to have simple expressions of useful accuracy for the rotor torque, X force, and Y force that are independent of the rotor blade angles. One such set of equations which take into account all the principal variables including the primary effects of the reverse-flow region may be obtained from a consideration of the distribution of the blade circulation. It may be noted before proceeding that the use of any radial blade-circulation distribution other than the uniform value assumed in the derivation of the induced-velocity equations will underestimate the induced torque. Thus, it is theoretically incorrect to calculate the induced torque from blade-element equations. However, for the extreme case of a triangular distribution of circulation along the radius and $\mu_v = 0.5$, the error in the induced torque is only $3\frac{1}{3}$ percent and thus is probably within the errors of present equations for the induced velocity.

For the present purposes a triangular distribution of blade circulation along the radius and a sinusoidal variation with azimuth angle is sufficiently accurate and will be used. Then

$$\Gamma = (\Gamma_0 + \Gamma_1 \sin \psi)x \tag{9}$$

Writing

$$U \cos \phi_v = \Omega R(x + \mu_v \sin \psi) \tag{10}$$

and

$$U \sin \phi_v = \Omega R\left[\lambda_v + yx \sin \psi + (wx - a_0\mu_v)\cos \psi\right] \tag{11}$$

it follows for thrust and rolling-moment equilibrium that

$$\Gamma = \frac{3\pi\Omega R^2 C_T}{b(1 - \mu_v^2)}\left(1 - \frac{4}{3}\mu_v \sin \psi\right)x \tag{12}$$

The reference blade angle A_0 at $r = 0.75R$ corresponding to the average value of the circulation and inflow angle at this station and a weighted chord may be obtained from the substitution

$$2\pi\alpha_{0.75R} = (c_l)_{0.75R} = 2(\Gamma/cU)_{0.75R}$$

or

$$A_0 = \sin^{-1}\left[\frac{C_T}{\pi b\sigma_3(1 - \mu_v^2)}\left(1 + \frac{16}{9}\mu_v^2 + \frac{64}{27}\mu_v^4 + \frac{2560}{729}\mu_v^6\right)\right] - \tan^{-1}\left(\frac{4}{3}\lambda_v\right) \tag{13}$$

where

$$\sigma_n = \frac{1}{\pi R}\int_{x_1}^{1} cx^{n-1}\,dx \tag{14}$$

For linearly tapered blades the values of σ_n may be obtained by interpolation from table 1.

The values of a_1 and b_1 obtained from the differences in blade circulation and inflow angle at $r = 0.75R$ for $\psi = \pi/2$ and $\psi = 3\pi/2$ for a_1 and $\psi = 0$ and $\psi = \pi$ for b_1 are

$$a_1 = \frac{\gamma - \frac{16}{9}\lambda_v\mu_v}{\left(1 - \frac{4}{3}\mu_v\right)^2} + \frac{8C_T\mu_v}{3\pi b\sigma_3\left(1 - \frac{25}{9}\mu_v^2 + \frac{16}{9}\mu_v^4\right)} \tag{15}$$

and

$$b_1 = -w + \frac{4}{3}a_0\mu_v \tag{16}$$

where the value of a_0 for blade root moment equilibrium on a blade with the flapping hinge at the axis of rotation is approximately

$$a_0 = \frac{3\rho\pi R^5 C_T\left(1 - \frac{8}{9}\mu_v^2\right)}{4bI_1(1 - \mu_v^2)} \tag{17}$$

Similarly

$$a_2 = \frac{8a_0\mu_v^2}{9 - 8\mu_v^2} \tag{18}$$

and

$$b_2 = 0 \tag{19}$$

The value of the blade-element profile-drag coefficient may be represented with sufficient accuracy for the present purposes by two terms in a power series in the blade-element lift coefficient c_l such that

$$c_{d_o} = \delta_0 + \epsilon c_l^2 \tag{20}$$

where for conventional airfoils $\delta_0 \approx 0.0080$ and $\epsilon \approx 0.0080$. Making the necessary substitutions and integrations the value of the rotor torque coefficient is

$$C_Q = \frac{C_T\left(\frac{1}{2} y\mu_v - \lambda_v\right)}{1 - \mu_v^2} + \frac{1}{2} b\delta_0 \left[\sigma_4 + \frac{1}{2}(\lambda_v^2 + \mu_v^2)\sigma_2\right] +$$

$$\frac{\epsilon}{2}\left(\frac{2C_T}{b\sigma_3}\right)^2 \frac{\left(1 + \frac{8}{9}\mu_v^2\right)b\sigma_4}{(1 - \mu_v^2)^2} + \Delta C_{Q_s} \quad \text{from equation (89b) (where applicable)} \tag{21}$$

Similarly, neglecting blade-shank drag which is assumed to be included in the helicopter parasite drag, the values of the X- and Y-force coefficients are

$$C_x = \frac{F_x}{\frac{1}{2}\rho\pi\Omega^2 R^4}$$

$$= \frac{C_T(2\lambda_v\mu_v - y)}{1 - \mu_v^2} + b\delta_0\mu_v\sigma_2 - \frac{\frac{4}{3}\epsilon b\mu_v\sigma_3\left(\frac{2C_T}{b\sigma_3}\right)^2}{(1 - \mu_v^2)^2} \tag{22}$$

and

$$C_y = \frac{F_y}{\frac{1}{2}\rho\pi\Omega^2 R^4} = \frac{C_T\left(w - \frac{3}{2} a_0\mu_v\right)}{1 - \mu_v^2} \tag{23}$$

The above equations based upon a triangular distribution of blade circulation along the radius and a sinusoidal variation with azimuth

angle are sufficiently accurate for preliminary calculations, checking, and the determination of the angle of attack and lateral tilt of the tip-path plane provided there are no large areas of the rotor outside the reverse-flow region that have blade elements operating in the stalled or negative thrust range. This implies a reasonable blade twist for the flight conditions.

Table 6 shows a comparison of the values of the parameters calculated from the above circulation equations with the flight test results of reference 2.

Determination of Angle of Attack and Lateral Tilt of Tip-Path Plane

Given the values of the flight-path velocity V, climb angle ϕ_c, gross weight and vertical component of the inertia force W, fuselage and wing drag, lift, moment characteristics, and position of center of gravity, the fuselage angle of attack and thus the fuselage and wing lift L_F and drag D_F can be obtained for the trim condition by setting the summation of moments, acting on the fuselage and wing and taken about the rotor hub, equal to zero. Since the lateral tilt of the tip-path plane has a negligible effect, it follows from the geometry of the above forces, as shown in figure 2, that

$$\tan \theta_y = - \frac{D_F \cos \phi_c - L_F \sin \phi_c + F_x \cos \theta_y}{W - L_F \cos \phi_c - D_F \sin \phi_c + F_x \sin \theta_y} \qquad (24)$$

is a good approximation for unaccelerated flight. It may be noted that D_F should include an allowance for rotor-hub and blade-shank drag. In general, the terms involving F_x will have only a small effect on the value of θ_y and a sufficiently exact solution can be obtained on the second iteration. Thus, as a first approximation,

$$\tan \theta_y = -\frac{D_F \cos \phi_c - L_F \sin \phi_c}{W - L_F \cos \phi_c - D_F \sin \phi_c} \tag{25}$$

$$\alpha_v = \phi_c + \theta_y \tag{26}$$

$$C_T = \frac{W - L_F \cos \phi_c - D_F \sin \phi_c}{\rho \pi \Omega^2 R^4 \cos \theta_y} \tag{27}$$

$$\mu_v = \frac{V \cos \alpha_v}{\Omega R} \tag{28}$$

$$\lambda_v = \frac{V \sin \alpha_v}{\Omega R} - \frac{v}{\Omega R} \tag{29}$$

The values of $v/\Omega R$ may be obtained from equation (2) or by double interpolation from table 7 which includes the experimental values for vertical descent from reference 3 and estimates of the values for the inclined flight "vortex ring" states. The values of w, y, and F_x can then be determined from equations (4), (5), and (22), and from these second approximations to the values of θ_y, α_v, and μ_v can be made from equations (24), (26), and (28). If necessary, a new value of C_T may then be obtained from the equation

$$C_T = \frac{W - L_F \cos \phi_c - D_F \sin \phi_c + F_x \sin \theta_y}{\rho \pi \Omega^2 R^4 \cos \theta_y} \tag{30}$$

and thus the more exact value of λ_v from equation (29).

For helicopter calculations the first approximation for C_T is sufficiently accurate, and if μ_v is small (i.e., $\mu_v < 0.15$) the effect of F_x on α_v may be neglected for level flight.

The tail-rotor thrust T_T required for a helicopter with a single main rotor is

$$T_T = Q/l \tag{31}$$

where l is the perpendicular distance between axis of main and tail rotors and the value of C_Q may be obtained from equation (21). The lateral tilt θ_x of the tip-path plane for a single-rotor aircraft in unaccelerated flight is thus

$$\theta_x \approx \frac{\frac{1}{2} C_y + C_Q \frac{R}{l}}{C_T} \tag{32}$$

where C_y is given by equation (23).

Application of Two-Dimensional Airfoil Theory and Data to Rotor-Blade-Element Calculations

Two-dimensional thin-airfoil theory demonstrates that

$$c_l = a \sin \alpha \tag{33}$$

For a two-dimensional cascade of airfoils, equation (33) is modified by a multiplying function of the solidity, chord spacing, and blade angles that is very nearly unity for average lifting-rotor configurations as shown in reference 4. Thus, within the approximation that the radial components of flow may be neglected, equation (33) should be applicable for blade-element rotor theory over the unstalled range of blade-element angles of attack. Beyond the stall, equation (33) is somewhat less in error than the usual relation $c_l = a\alpha$ as can be seen from figure 3 which is a plot of the above expressions and the experimental values of c_l against α for an NACA 0015 airfoil. The use of equation (33), rather than the usual approximation that $c_l = a\alpha$, allows the thrust and tangential components of lift on a blade element to be exactly expressed, within the approximations involved in neglecting radial components of the flow, in terms of the easily integrated in-plane and normal components of the velocity at the blade element $U \cos \phi_v$ and $U \sin \phi_v$. Thus the usual approximation that the inflow angle ϕ_v is a small angle may be eliminated. This may be demonstrated as follows:

Omitting the negligible component of the profile drag, the thrust dT on a blade element $c\,dr$ is

$$dT = \frac{1}{2}\rho U^2 c c_l \cos \phi_v \, dr \tag{34}$$

or since

$$c_l = a \sin \alpha_r = a\left(\sin \theta_v \cos \phi_v + \cos \theta_v \sin \phi_v\right) \tag{35}$$

$$dT = \frac{1}{2}\rho a c\left(U \cos \phi_v\right)\left[\sin \theta_v\left(U \cos \phi_v\right) + \cos \theta_v\left(U \sin \phi_v\right)\right] dr \tag{36}$$

The tangential component of the lift on a blade element may be similarly expressed as

$$dL \sin \phi_v = \frac{1}{2}\rho a c\left(U \sin \phi_v\right)\left[\sin \theta_v\left(U \cos \phi_v\right) + \cos \theta_v\left(U \sin \phi_v\right)\right] dr \tag{37}$$

The value of the slope of the lift curve a of the blade-element airfoil in the above relations may be taken as the value corresponding to the Reynolds number, Mach number, and surface roughness existing at the three-quarter-radius point of the rotor blades under consideration. For the usual tip speeds, in the 500-foot-per-second range, the Prandtl-Glauert Mach number correction

$$a = \frac{a'}{\sqrt{1 - M^2}} \tag{38}$$

where

a' low Mach number lift-curve slope from two-dimensional wind-tunnel tests

M free-stream Mach number at three-quarter blade radius

may be used to correct the lift-curve slope from low Mach number data.

The values of c_{d_o} obtained from two-dimensional wind-tunnel tests at appropriate Reynolds numbers and model surface roughness should be

directly applicable to rotor-blade-element calculations in the unstalled range of angles of attack below the Mach numbers and angles of attack for drag divergence, since the effect of subsonic Mach number on profile drag is negligible as shown in reference 5. However, it should be noted that the profile-drag coefficient is only constant with change of subsonic Mach number if it is taken as a function of the lift coefficient. If the airfoil section data are plotted against section angle of attack and the Prandtl-Glauert correction is applied to the lift-curve slope, this is equivalent to multiplying the section-angle-of-attack scale by $(1 - M^2)^{1/2}$. Consequently, the section-angle-of-attack scale on the profile-drag curve must be multiplied by $(1 - M^2)^{1/2}$ to retain the same relation between c_{d_o} and c_l.

In view of the errors in the magnitude and distribution of the blade circulation that arise from the necessary neglect of blade deflections, and so forth, it is probably not justifiable to take into account secondary effects of the profile drag. Thus, expressing the relation between the profile-drag coefficient and the blade-element angle of attack by the first three terms of a Fourier series gives

$$c_{d_o} = \epsilon_0 + \epsilon_1 \sin \alpha_r + \epsilon_2 \cos \alpha_r \tag{39}$$

The constants in the above equation may be evaluated from the two-dimensional wind-tunnel data for the blade airfoil at, say, $\alpha = 0^\circ$, 5°, and 10°. The advantages of equation (39) over the usual expression

$$c_{d_o} = \delta_0 + \delta_1 \alpha_r + \delta_2 \alpha_r^2$$

are: The last two terms of equation (39) can be exactly expressed in the known velocity components $U \cos \phi_v$ and $U \sin \phi_v$; the resulting expressions for the forces and moments on the blade are considerably simplified by the absence of the squared term in α_r; and it is an equally accurate approximation to the experimental values of c_{d_o} as may be seen from figure 4. However, in using equation (39) it may be noted that the calculated value of c_{d_o} is the small difference between large quantities and thus the values of ϵ_0, ϵ_1, and ϵ_2 should be determined to four places in order to obtain the value of c_{d_o} to the customary accuracy. For the more severe convertaplane flight conditions where the inflow velocity is large $(|\lambda_v| > 0.10)$ a certain error arises in the treatment of the ϵ_0 terms, and it is necessary to fall back on

the two-term approximation for c_{d_o}, $c_{d_o} = \epsilon_1 \sin \alpha_r + \epsilon_2 \cos \alpha_r$, where ϵ_1 and ϵ_2 are evaluated from the experimental data at, say, $\alpha = 2^\circ$ and $\alpha = 7^\circ$. This additional approximation is permissible for these flight conditions, since the relative effects of the profile drag become less important as the inflow velocities and rotor blade angles increase. For example, in propeller calculations the single-point approximation $c_{d_o} = \epsilon c_l$ is usually used.

It follows from the geometry and equations (35) and (39) that the tangential component of the profile drag on a blade element may be expressed as

$$dD_o \cos \phi_v = \frac{1}{2} \rho c (U \cos \phi_v) \left\{ \epsilon_0 U + \epsilon_1 \left[(U \cos \phi_v) \sin \theta_v + (U \sin \phi_v) \cos \theta_v \right] + \epsilon_2 \left[(U \cos \phi_v) \cos \theta_v - (U \sin \phi_v) \sin \theta_v \right] \right\} dr \tag{40}$$

Thrust of a Blade at Azimuth Angle ψ

The thrust F_z of a blade at azimuth angle ψ is

$$F_z = \frac{1}{2} \rho a \int_{r_1}^{R} c (U \cos \phi_v) \left[(U \cos \phi_v) \sin \theta_v + (U \sin \phi_v) \cos \theta_v \right] dr \tag{41}$$

where r_1 is the radius of the inboard blade airfoil element. In the general case it follows from the geometry that

$$U \cos \phi_v = \Omega R (x + \mu_v \sin \psi) \tag{42}$$

and

$$U \sin \phi_v = \Omega R \left[\lambda_v + (wx + \omega_y x - a_0 \mu_v) \cos \psi + (y - \omega_x) x \sin \psi + 2b_2 x \cos 2\psi - 2a_2 x \sin 2\psi \right] \tag{43}$$

where

ω_x ratio of angular velocity of roll of tip-path plane about X-axis to Ω

ω_y ratio of angular velocity of pitch of tip-path plane about Y-axis to Ω

Neglecting the higher harmonics of the cyclic pitch that may arise from control-system linkages, the pitch angle θ_v of a blade element at radius r and aximuth angle ψ, measured with respect to the tip-path plane, is

$$\theta_v = A_0 + \theta_t - a_1 \sin \psi + b_1 \cos \psi \tag{44}$$

where

A_0 mean blade pitch angle at reference station

θ_t twist in rotor blade angle of zero lift between reference station and radius r

a_1 minus the coefficient of sine component of blade cyclic-pitch angle measured with respect to tip-path plane

b_1 coefficient of cosine component of cyclic-pitch angle measured with respect to tip-path plane

In the general case (i.e., for the convertaplane) A_0 and θ_t may not be small angles. However, it appears that the magnitude of the cyclic-pitch angle will always be limited by tip stall on the retreating blade to the range where it is a good approximation that

$$\sin \left(-a_1 \sin \psi + b_1 \cos \psi\right) = -a_1 \sin \psi + b_1 \cos \psi \tag{45}$$

and

$$\cos \left(-a_1 \sin \psi + b_1 \cos \psi\right) = 1 \tag{46}$$

It follows from equation (44), upon expanding the functions $\sin \theta_v$ and $\cos \theta_v$, that

$$\sin \theta_v = \left[\sin A_0 + \left(\cos A_0\right)\left(-a_1 \sin \psi + b_1 \cos \psi\right)\right] \cos \theta_t + \left[\cos A_0 - \left(\sin A_0\right)\left(-a_1 \sin \psi + b_1 \cos \psi\right)\right] \sin \theta_t \tag{47}$$

$$\cos \theta_v = \left[\cos A_0 - \left(\sin A_0\right)\left(-a_1 \sin \psi + b_1 \cos \psi\right)\right] \cos \theta_t - \left[\sin A_0 + \left(\cos A_0\right)\left(-a_1 \sin \psi + b_1 \cos \psi\right)\right] \sin \theta_t \tag{48}$$

Substituting the values of $U \cos \phi_v$, $U \sin \phi_v$, $\sin \theta_v$, and $\cos \theta_v$ from equations (42), (43), (47), and (48) in equation (41), defining

$$\sigma_{nc} = \frac{1}{\pi R} \int_{x_1}^{1} c x^{n-1} \cos \theta_t \, dx \tag{49}$$

$$\sigma_{ns} = \frac{1}{\pi R} \int_{x_1}^{1} c x^{n-1} \sin \theta_t \, dx \tag{50}$$

$$I_{nc} = \sigma_{nc} \sin A_0 + \sigma_{ns} \cos A_0 \tag{51}$$

$$I_{ns} = \sigma_{ns} \sin A_0 - \sigma_{nc} \cos A_0 \tag{52}$$

multiplying out the terms, and reducing the functions of ψ to harmonic form give for the thrust coefficient $C_z = \frac{F_z}{\frac{1}{2} \rho \pi \Omega^2 R^4}$ of one blade at an azimuth angle ψ the expression of equation (53):

C_x/a =

Equation (53)

	I_{3c}	I_{2c}	I_{1c}	I_{3s}	I_{2s}	I_{1s}
1	$1 + \frac{1}{2}a_1(y - \omega_x) - \frac{1}{2}b_1(w + \omega_y)$	$\frac{1}{2}(a_0 + a_2)b_1\mu_v - \frac{1}{2}a_1b_2\mu_v$	$\frac{1}{2}(a_1\lambda_v + \mu_v)\mu_v$	$\frac{1}{2}(a_1a_2 + b_1b_2)(w + \omega_y) + \frac{1}{2}(a_1b_2 - a_2b_1)(y - \omega_x)$	$a_1\mu_v - \lambda_v - \frac{1}{2}(y - \omega_x)\mu_v - \frac{1}{2}(a_1a_2 + b_1b_2)a_0\mu_v$	
$\sin\psi$	$a_2(b_1 + w + \omega_y) - b_2(a_1 - y + \omega_x)$	$(2 - a_0a_2)\mu_v + a_1\lambda_v + \frac{3}{4}a_1(y - \omega_x)\mu_v - \frac{1}{4}b_1(w + \omega_y)\mu_v$	$\frac{1}{4}a_0b_1\mu_v^2$	$a_1 - (y - \omega_x)$	$(a_1b_2 - a_2b_1)\lambda_v + b_2\mu_v$	$\left(\frac{1}{4}a_1\mu_v - \lambda_v\right)\mu_v$
$\cos\psi$	$-a_2(a_1 - y + \omega_x) - b_2(b_1 + w + \omega_y)$	$a_0b_2\mu_v - b_1\lambda_v + \frac{1}{4}a_1(w + \omega_y)\mu_v - \frac{1}{4}b_1(y - \omega_x)\mu_v$	$-\frac{1}{4}a_0a_1\mu_v^2$	$-b_1 - (w + \omega_y)$	$(a_0 + a_2)\mu_v + (a_1a_2 + b_1b_2)\lambda_v$	$-\frac{1}{4}b_1\mu_v^2$
$\sin 2\psi$	$-\frac{1}{2}a_1(w + \omega_y) - \frac{1}{2}b_1(y - \omega_x)$	$-\left(\frac{1}{2}a_0 + a_2\right)a_1\mu_v + 2a_2\lambda_v$	$-\frac{1}{2}b_1\lambda_v\mu_v$	$2a_2 + a_1a_2(y - \omega_x) - a_2b_1(w + \omega_y)$	$(a_0a_2 - 1)b_1\mu_v - \frac{1}{2}(w + \omega_y)\mu_v$	$\frac{1}{2}a_0\mu_v^2$
$\cos 2\psi$	$-\frac{1}{2}a_1(y - \omega_x) - \frac{1}{2}b_1(w + \omega_y)$	$\left(\frac{1}{2}a_0b_1 + a_1b_2\right)\mu_v - 2b_2\lambda_v$	$-\frac{1}{2}(a_1\lambda_v + \mu_v)\mu_v$	$-2b_2 - a_1b_2(y - \omega_x) + b_1b_2(w + \omega_y)$	$-(a_1 + a_0b_1b_2)\mu_v + \frac{1}{2}(y - \omega_x)\mu_v$	
$\sin 3\psi$		$-\frac{1}{4}a_1(y - \omega_x)\mu_v - \frac{1}{4}b_1(w + \omega_y)\mu_v$	$\frac{1}{4}a_0b_1\mu_v^2$			$-\frac{1}{4}a_1\mu_v^2$
$\cos 3\psi$		$-\frac{1}{4}a_1(w + \omega_y)\mu_v + \frac{1}{4}b_1(y - \omega_x)\mu_v$	$\frac{1}{4}a_0a_1\mu_v^2$			$\frac{1}{4}b_1\mu_v^2$

Equation (53) is written in tabular form where the coefficients in the boxes must be multiplied by row and column heads. Values of σ_{nc} and σ_{ns} may be obtained by interpolation from tables 2 and 3 for linearly tapered and twisted blades, where

$$c = c_o(1 + tx) \quad \text{from} \quad x = 0.15 \quad \text{to} \quad x = 1 \tag{54}$$

$$\theta_t = \theta_1 x \tag{55}$$

$$\sigma_0 = \frac{c_o}{\pi R} \tag{56}$$

and

c_o extended blade-root chord at $r = 0$

$t = \dfrac{\text{Tip chord}}{c_o} - 1$

θ_1 twist in angle of blade zero lift between axis of rotation and tip

In order to use the tabulated values of σ_{nc} and σ_{ns} for blades with linear twist and taper, it is necessary to take the reference blade pitch angle A_0 at the extended blade-root chord c_o at $r = x = 0$.

The use of the lower limit $x_1 = 0.15$ in the computations for the blades having linear taper and twist corresponds to present practice and largely eliminates the necessity of making any reverse-flow correction to the blade thrust. The reverse-flow effects are discussed in the following section.

Additional tables (tables 4 and 5) give the values of σ_{nc} and σ_{ns} for blades having linear taper from $x_1 = 0.20$ to $x = 1$ and helical twist where

$$\theta_t = \tan^{-1}\left(\frac{\tan \theta_T}{x}\right) \tag{57}$$

and θ_T is the design helix angle at $x = 1$. In this case, the reference station for A_0 is taken at the blade tip. The tables for helical twist are included for convertaplane usage since helical twist would appear to be desirable for a reasonable propeller efficiency. An inner limit of $x_1 = 0.20$ was used for the computation of the values of σ_{nc} and σ_{ns} for this case of helical twist in order to minimize the severe root stall likely to occur under some convertaplane flight conditions. It might be pointed out that helical twist would also appear to afford an increase in helicopter-rotor performance over that obtainable with linear twist.

Reverse-Flow Considerations

For normal helicopter and convertaplane flight conditions where there is a downflow through the rotor and ϕ_v is negative over the reverse-flow region, the maximum value of μ_v is limited for conventional rotors to relatively low values of the order of 0.30 by tip stall on the retreating blades. Under these conditions the portion of the retreating blade extending inboard from the outer edge of the reverse-flow region at $x = -\mu_v \sin \psi$, where the in-plane component of velocity is zero, to $x = x_1$, where the blade airfoil section ends, has a negligible thrust loading because the in-plane components of velocity are very small. The present equations take into account the fact that the blade airfoil does not exist inboard of $x = x_1$, for which region the the in-plane components of velocity are larger, within the reverse-flow circle, and previous equations erred in assuming the blade airfoil to exist.

For those flight conditions where there is an upflow through the rotor and the tip-stall limitations on μ_v are relaxed, the present equations give the proper direction to the blade-element thrust for those blade elements within the reverse-flow region and inside the radius where $\phi_v \approx 2\theta_v$.

Thus, for all practical purposes, it is not necessary to use reverse-flow corrections when applying the present equations to conventional rotors.

For unconventional rotors operating with net downflow at large values of μ_v it would appear from strip analysis to be desirable and even necessary to minimize the forces in the reverse-flow region by using a sufficiently large design value of x_1, for example, $x_1 > \frac{1}{2}\mu_{v_{max}}$. In this case less error is introduced by taking into account the inboard blade airfoil limit and omitting the usual reverse-flow correction than vice versa.

Mean Rotor Thrust

Omitting the coefficients of the second-harmonic flapping angle which have a negligible effect on the mean rotor thrust, the value of the mean rotor thrust coefficient obtained from the first row of equation (53) by averaging the value of C_z/a over the interval from $\psi = 0$ to $\psi = 2\pi$ is given by

$$\frac{2C_T}{ab} = \left[1 + \frac{1}{2}a_1(y - \omega_x) - \frac{1}{2}b_1(w + \omega_y)\right]I_{3c} + \frac{1}{2}a_0b_1\mu_v I_{2c} +$$

$$\frac{1}{2}(a_1\lambda_v + \mu_v)\mu_v I_{1c} - \left[\lambda_v - a_1\mu_v + \frac{1}{2}(y - \omega_x)\mu_v\right]I_{2s} \qquad (58)$$

Mean Rotor Air Rolling Moment

The value of the mean rotor air-rolling-moment coefficient about the X-axis

$$C_{mx} = \frac{M_x}{\frac{1}{2}\rho\pi\Omega^2R^5}$$

is found, upon integration, to be obtained by multiplying the second row of equation (53) by $\frac{1}{2}b$ and introducing the moment arm by writing the subscripts of I_{nc} and I_{ns} to one higher order. Thus,

$$\frac{2C_{mx}}{ab} = \left[2\mu_v + a_1\lambda_v + \frac{3}{4}a_1(y - \omega_x)\mu_v - \frac{1}{4}b_1(w + \omega_y)\mu_v\right]I_{3c} +$$

$$\frac{1}{4}a_0b_1\mu_v^2I_{2c} + (a_1 - y + \omega_x)I_{4s} + \left(\frac{3}{4}a_1\mu_v - \lambda_v\right)\mu_v I_{2s} \qquad (59)$$

Mean Rotor Air Pitching Moment

Similarly, the mean rotor air-pitching-moment coefficient

$$C_{my} = \frac{M_y}{\frac{1}{2}\rho\pi\Omega^2R^5}$$

obtained from the third row of equation (53) is

$$\frac{2C_{my}}{ab} = \left[b_1\lambda_v - \frac{1}{4}a_1(w + \omega_y)\mu_v + \frac{1}{4}b_1(y - \omega_x)\mu_v\right]I_{3c} +$$

$$\frac{1}{4}a_0a_1\mu_v{}^2I_{2c} + (b_1 + w + \omega_y)I_{4s} - a_0\mu_vI_{3s} + \frac{1}{4}b_1\mu_v{}^2I_{2s} \qquad (60)$$

Mean Blade-Root Air Moment

The coefficient C_{mo} of the blade-root air moment M_o is merely the first row of equation (53) with the I factors to one higher subscript. Thus, for

$$C_{mo} = \frac{M_o}{\frac{1}{2}\rho\pi\Omega^2R^5}$$

$$\frac{C_{mo}}{a} = \left[1 + \frac{1}{2}a_1(y - \omega_x) - \frac{1}{2}b_1(w + \omega_y)\right]I_{4c} + \frac{1}{2}a_0b_1\mu_vI_{3c} +$$

$$\frac{1}{2}(a_1\lambda_v + \mu_v)\mu_vI_{2c} - \left[\lambda_v - a_1\mu_v + \frac{1}{2}(y - \omega_x)\mu_v\right]I_{3s} \qquad (61)$$

Equilibrium Values of Mean Rotor Pitching Moment

and Rolling Moment

If an external moment M_1 is applied to a single rotor with three or more blades about a diameter, axis 1, the differential equations of motion about axis 1 at $\psi = \psi_1$ and axis 2 at $\psi = \psi_1 + 90^\circ$ can be shown by the use of Euler's equations to be

$$\frac{1}{2}\frac{d\omega_1}{dt} + \Omega\omega_2 + \frac{k_1\omega_1}{I_v} = \frac{M_1}{I_v} \qquad (62)$$

and

$$\frac{1}{2}\frac{d\omega_2}{dt} - \Omega\omega_1 + \frac{k_2\omega_2}{I_v} = 0 \tag{63}$$

where ω_1 and ω_2 are the angular velocities of the tip-path plane about axes 1 and 2, respectively, $k_1\omega_1$ and $k_2\omega_2$ are the damping moments, and I_v is the mass moment of inertia of the rotor about the virtual axis of rotation. The general solution of equations (62) and (63) is a pair of equations of the form

$$\omega_{1 \text{ or } 2} = \left[A \sin\sqrt{4\Omega^2 - \left(\frac{k_1 - k_2}{I_v}\right)^2}\,t + B \cos\sqrt{4\Omega^2 - \left(\frac{k_1 - k_2}{I_v}\right)^2}\,t\right] e^{-\frac{k_1+k_2}{I_v}t} \tag{64}$$

In the actual case, damping of the nutation appears to be very rapid for an articulated rotor. Also, for pilot-controlled motion, $k_2 \approx 0$. For example, for a constant control moment M_1, $k_2 = 0$, and $k_1 = 2\Omega I_v$, which is then the value of k_1 for critical damping, it follows that

$$\omega_1 = \frac{2M_1 t}{I_v} e^{-2\Omega t} \tag{65}$$

or

$$\omega_2 = \frac{M_1}{I_v\Omega}\left(1 - e^{-2\Omega t}\right) \tag{66}$$

It can be seen from equations (65) and (66) that the transients decay very rapidly and their effects can be neglected in most problems. Therefore, to a good approximation for a single rotor

$$M_x = I_v\Omega^2\omega_y + M_{xf} \tag{67}$$

$$M_y = -I_v\Omega^2\omega_x + M_{yf} \tag{68}$$

where M_{xf} and M_{yf} are any moments transmitted about the X- and Y-axes from the fuselage to the rotor. For steady straight and level flight

$$\omega_x = \omega_y = 0 \tag{69}$$

For steady banked turns the value of C_T can be taken proportional to sec θ_x. Also

$$\omega_x \approx \frac{-g \sin \theta_y \tan \theta_x}{V\Omega} \tag{70}$$

and

$$\omega_y \approx \frac{g \sin \theta_x \tan \theta_x}{V\Omega} \tag{71}$$

where θ_x is the equilibrium lateral-tilt angle of the tip-path plane (approximately equal to equilibrium angle of bank, positive for turns in direction of rotor rotation).

For any curvature of the flight path, the nondimensional components ω_x and ω_y of the spatial angular velocity of the aircraft may be calculated and, consequently, the approximate equilibrium values of M_x and M_y can be obtained from equations (67) and (68).

Approximate Solution for Equilibrium Values of Mean Reference Blade Angle A_0, Lateral and Longitudinal Components of Cyclic Pitch a_1 and b_1, and Coning Angle a_0

An approximate solution of the set of four nonlinear, transcendental equations (58), (59), (60), and (61) for the four unknowns A_0, a_1, a_0, and b_1 that is sufficiently accurate for most steady-flight helicopter work and useful as a first trial for steady-flight convertaplane calculations may be obtained as follows: Setting the small terms and ω_x, ω_y, and C_{mx} equal to zero and $\cos A_0 = 1$ in equations (58) and (59) and eliminating a_1 gives

$$\sin A_0 = \frac{\left(\frac{2C_T}{ab} - \sigma_{3s} - \lambda_v\sigma_{2c}\right)\left(\sigma_{4c} + \frac{3}{4}\mu_v^2\sigma_{2c} - \lambda_v\sigma_{3s}\right) + \mu_v^2\sigma_{2c}\left(2\sigma_{3s} + \lambda_v\sigma_{2c}\right)}{\left(\sigma_{3c} + \frac{1}{2}\mu_v^2\sigma_{1c} - \lambda_v\sigma_{2s}\right)\left(\sigma_{4c} + \frac{3}{4}\mu_v^2\sigma_{2c} - \lambda_v\sigma_{3s}\right) - 2\mu_v^2\sigma_{2c}\sigma_{3c}} \tag{72}$$

Then, from equation (59) for $\omega_x = \omega_y = C_{mx} = 0$

$$a_1 = -\frac{2\mu_v I_{3c} - yI_{4s} - \lambda_v \mu_v I_{2s}}{\left(\lambda_v + \frac{3}{4} y\mu_v\right) I_{3c} + I_{4s} + \frac{3}{4} \mu_v^2 I_{2s}} \tag{73}$$

Let $\bar{a}_0$ be the design coning angle for the general case of semirigid blades (i.e., coning angle for zero blade-root bending moment). Let k_{a_0} be the spring constant of the blade for angular deflections of the three-quarter-radius point from $\bar{a}_0$. Then setting the summation of moments about the blade root equal to zero and solving for a_0, the coning angle at the three-quarter-radius point,

$$a_0 \approx \frac{\frac{1}{2} \rho \pi a \Omega^2 R^5 \left[I_{4c} + \frac{1}{2}\left(a_1 \lambda_v + \mu_v\right)\mu_v I_{2c} - \left(\lambda_v - a_1 \mu_v\right) I_{3s} \right] + \bar{a}_0 k_{a_0} - M_B \bar{r} g}{I_1 \Omega^2 + k_{a_0}} \tag{74}$$

where

M_B mass of blade

$\bar{r}$ radius of blade center of gravity

I_1 mass moment of inertia of blade about flapping hinge (or root)

(If the blades have a flapping hinge at the axis of rotation $\bar{a}_0 = k_{a_0} = 0$. If the flapping hinge is located at radius r_β from the axis of rotation, $\bar{a}_0 = 0$ and $k_{a_0} \approx \frac{r_\beta \bar{r} M_B \Omega^2}{1 - \left(r_\beta / 0.75R\right)}$.) Then, knowing a_0, it follows from equation (60) that for

$$\omega_x = \omega_y = C_{my} = 0$$

$$b_1 \approx \frac{a_0 \mu_v I_{3s} - wI_{4s}}{\lambda_v I_{3c} + I_{4s} + \frac{1}{4} \mu_v^2 I_{2s}} \tag{75}$$

For those steady, unaccelerated flight conditions where $\cos A_0 \approx 1$, the above solutions are sufficiently accurate and may be used to calculate the blade loadings and rotor torque, X force, and Y force.

"Exact" Solution for A_0, a_1, and b_1 for Accelerated Flight Conditions and Those Flight Conditions where $\cos A_0 \neq 1$

A reasonably rapid and sufficiently accurate solution of the "exact" equilibrium equations given by the first three rows of equation (53) can be obtained by using an approximate value for the coning angle a_0 such as that given by equation (17) or (74).

Then for the approximate value of A_0 given by equation (72) and, for example, two other values several degrees successively smaller, the "exact" corresponding values of a_1 and b_1 can be determined by rewriting the equilibrium equations for the rotor pitching and rolling moments in the form

$$\left.\begin{aligned} Aa_1 + Bb_1 &= P - \frac{2C_{my}}{ab} \\ \text{and} \\ Ca_1 + Db_1 &= R + \frac{2C_{mx}}{ab} \end{aligned}\right\} \tag{76}$$

where

$$A = \frac{1}{4}(w + \omega_y)\mu_v I_{3c} - \frac{1}{4} a_0 \mu_v^2 I_{2c} \tag{77}$$

$$B = -\lambda_v I_{3c} - \frac{1}{4}(y - \omega_x)\mu_v I_{3c} - I_{4s} - \frac{1}{4}\mu_v^2 I_{2s} \tag{78}$$

$$C = \lambda_v I_{3c} + \frac{3}{4}(y - \omega_x)\mu_v I_{3c} + I_{4s} + \frac{3}{4}\mu_v^2 I_{2s} \tag{79}$$

$$D = -\frac{1}{4}(w + \omega_y)\mu_v I_{3c} + \frac{1}{4} a_0 \mu_v^2 I_{2c} \tag{80}$$

$$P = (w + \omega_y) I_{4s} - a_0 \mu_v I_{3s} \tag{81}$$

$$R = -2\mu_v I_{3c} + (y - \omega_x) I_{4s} + \lambda_v \mu_v I_{2s} \tag{82}$$

Then

$$a_1 = \frac{\begin{vmatrix} \left(P - \frac{2C_{my}}{ab}\right) & B \\ \left(R + \frac{2C_{mx}}{ab}\right) & D \end{vmatrix}}{\begin{vmatrix} A & B \\ C & D \end{vmatrix}} \tag{83}$$

and

$$b_1 = \frac{\begin{vmatrix} A & \left(P - \frac{2C_{my}}{ab}\right) \\ C & \left(R + \frac{2C_{mx}}{ab}\right) \end{vmatrix}}{\begin{vmatrix} A & B \\ C & D \end{vmatrix}} \tag{84}$$

Having computed the values of a_1 and b_1 for each of the assumed values of A_0, the corresponding values of C_T may be found from the equation for the thrust equilibrium where

$$\frac{2C_T}{ab} = I_{3c} + \frac{1}{2}\mu_v^2 I_{1c} - \lambda_v I_{2s} - \frac{1}{2}(y - \omega_x)\mu_v I_{2s} +$$

$$\left[\frac{1}{2}(y - \omega_x) I_{3c} + \frac{1}{2}\lambda_v \mu_v I_{1c} + \mu_v I_{2s}\right] a_1 +$$

$$\left[\frac{1}{2} a_0 \mu_v I_{2c} - \frac{1}{2}(w + \omega_y) I_{3c}\right] b_1 \tag{85}$$

Then plotting the values of $2C_T/ab$, a_1, and b_1 against the trial values of A_0, the "exact" value of A_0, and thus a_1 and b_1, may be obtained from the plot at the design or desired value of C_T.

In-Plane Component of Force F_{xy} on a Blade at Azimuth Angle ψ

The in-plane component of force in the direction of rotation F_{xy} on a blade at azimuth angle ψ is from equations (37) and (40)

$$F_{xy} = \frac{1}{2}\rho a \int_{r_1}^{R} c\left(U \sin \phi_v\right)\left[\sin \theta_v\left(U \cos \phi_v\right) + \cos \theta_v\left(U \sin \phi_v\right)\right] dr -$$

$$\frac{1}{2}\rho \int_{r_1}^{R} c\left(U \cos \phi_v\right)\left\{\epsilon_0 U + \epsilon_1\left[\sin \theta_v\left(U \cos \phi_v\right) +\right.\right.$$

$$\left.\left.\cos \theta_v\left(U \sin \phi_v\right)\right] + \epsilon_2\left[\cos \theta_v\left(U \cos \phi_v\right) - \sin \theta_v\left(U \sin \phi_v\right)\right]\right\} dr \tag{86}$$

where

$$c_{d_o} = \epsilon_0 + \epsilon_1 \sin \alpha_r + \epsilon_2 \cos \alpha_r$$

Then, by (1) substituting the previously evaluated expressions for $U \cos \phi_v$, $U \sin \phi_v$, $\sin \theta_v$, and $\cos \theta_v$ given by equations (42), (43), (47), and (48); (2) neglecting the effects of second-harmonic flapping; and (3) writing $(\epsilon_0 U)(U \cos \phi_v)$ as $\epsilon_0 (U \cos \phi_v)^2 (U/U \cos \phi_v)$ and expanding

$$\frac{U}{U \cos \phi_v} = \sqrt{1 + \left(\frac{U \sin \phi_v}{U \cos \phi_v}\right)^2}$$

by the binomial theorem and dropping third and higher terms, the expression for the constant and first-harmonic terms becomes

$$C_{xy} = \frac{F_{xy}}{\frac{1}{2}\rho \pi \Omega^2 R^4} = \left(\Delta C_{xy}\right)_a - \left(\Delta C_{xy}\right)_{\epsilon_0} - \left(\Delta C_{xy}\right)_{\epsilon_1} - \left(\Delta C_{xy}\right)_{\epsilon_2} \tag{87}$$

where

$$\frac{(\Delta\omega_{xy})_a}{a} =$$

	I_{3c}	I_{2c}	I_{1c}	I_{3s}	I_{2s}	I_{1s}
1		$\lambda_v + \frac{1}{2}(y - \omega_x)\mu_v + a_1(y - \omega_x)\lambda_v - b_1(w + \omega_y)\lambda_v$	$a_0 b_1 \lambda_v \mu_v$	$\frac{1}{2} a_1(y - \omega_x) - \frac{1}{2} b_1(w + \omega_y) - \frac{1}{2}(y - \omega_x)^2 - \frac{1}{2}(w + \omega_y)^2$	$\frac{1}{2} a_0 b_1 \mu_v + a_0(w + \omega_y)\mu_v$	$\frac{1}{2} a_1 \lambda_v \mu_v - \lambda_v^2 - \frac{1}{2} a_0^2 \mu_v^2$
$\sin \Psi$	$y - \omega_x + \frac{3}{4} a_1(y - \omega_x)^2 - \frac{1}{2} b_1(y - \omega_x)(w + \omega_y) + \frac{1}{4} a_1(w + \omega_y)^2$	$\frac{1}{2} a_0 b_1(y - \omega_x)\mu_v - \frac{1}{2} a_0 a_1(w + \omega_y)\mu_v$	$(a_1 \lambda_v + \mu_v)\lambda_v + \frac{1}{4} a_0^2 a_1 \mu_v^2$		$(a_1 - 2y + 2\omega_x)\lambda_v + \frac{3}{4} a_1(y - \omega_x)\mu_v - \frac{1}{4} b_1(w + \omega_y)\mu_v$	$\frac{1}{4} a_0 b_1 \mu_v^2$
$\cos \Psi$	$w + \omega_y - \frac{1}{4} b_1(y - \omega_x)^2 + \frac{1}{2} a_1(y - \omega_x)(w + \omega_y) - \frac{3}{4} b_1(w + \omega_y)^2$	$-a_0 \mu_v - \frac{1}{2} a_0 a_1(y - \omega_x)\mu_v + \frac{3}{2} a_0 b_1(w + \omega_y)\mu_v$	$-b_1 \lambda_v^2 - \frac{3}{4} a_0^2 b_1 \mu_v^2$		$\frac{1}{4} a_1(w + \omega_y)\mu_v - b_1 \lambda_v - \frac{1}{4} b_1(y - \omega_x)\mu_v - 2(w + \omega_y)\lambda_v$	$-\frac{1}{4} a_0 a_1 \mu_v^2 + 2 a_0 \lambda_v \mu_v$

(88a)

$$\frac{(\Delta\omega_{xy})_{\epsilon_0}}{\epsilon_0} =$$

	σ_3	σ_2	σ_1
1	$1 + \frac{1}{4}(w + \omega_y)^2 + \frac{1}{4}(y - \omega_x)^2$	$-\frac{1}{2} a_0(w + \omega_y)\mu_v$	$\frac{1}{2}\left[\lambda_v^2 + \left(1 + \frac{1}{2} a_0^2\right)\mu_v^2\right]$
$\sin \Psi$		$(y - \omega_x)\lambda_v + 2\mu_v$	
$\cos \Psi$		$(w + \omega_y)\lambda_v$	$-a_0 \lambda_v \mu_v$

(88b)

$$\frac{(\Delta C_{xy})_{\epsilon_1}}{\epsilon_1} =$$

	I_{3c}	I_{2c}	I_{1c}	I_{3s}	I_{2s}	I_{1s}
1	$1 + \frac{1}{2} a_1(y - \omega_x) - \frac{1}{2} b_1(w + \omega_y)$	$\frac{1}{2} a_0 b_1 \mu_v$	$\frac{1}{2}(a_1\lambda_v + \mu_v)\mu_v$		$a_1\mu_v - \lambda_v - \frac{1}{2}(y - \omega_x)\mu_v$	
sin ψ		$2\mu_v + a_1\lambda_v + \frac{3}{4} a_1(y - \omega_x)\mu_v - \frac{1}{4} b_1(w + \omega_y)\mu_v$	$\frac{1}{4} a_0 b_1 \mu_v^2$	$a_1 - (y - \omega_x)$		$\left(\frac{3}{4} a_1\mu_v - \lambda_v\right)\mu_v$
cos ψ		$\frac{1}{4} a_1(w + \omega_y)\mu_v - \frac{1}{4} b_1(y - \omega_x)\mu_v - b_1\lambda_v$	$-\frac{1}{4} a_0 a_1 \mu_v^2$	$-b_1 - (w + \omega_y)$	$a_0\mu_v$	$-\frac{1}{4} b_1\mu_v^2$

(88c)

and

$$\frac{(\Delta C_{xy})_{\epsilon_2}}{\epsilon_2} =$$

	I_{3c}	I_{2c}	I_{1c}	I_{3s}	I_{2s}	I_{1s}
1		$a_1\mu_v - \lambda_v - \frac{1}{2}(y - \omega_x)\mu_v$		$-1 - \frac{1}{2} a_1(y - \omega_x) + \frac{1}{2} b_1(w + \omega_y)$	$-\frac{1}{2} a_0 b_1 \mu_v$	$-\frac{1}{2}(a_1\lambda_v + \mu_v)\mu_v$
sin ψ	$a_1 - (y - \omega_x)$		$\left(\frac{3}{4} a_1\mu_v - \lambda_v\right)\mu_v$		$-2\mu_v - a_1\lambda_v - \frac{3}{4} a_1(y - \omega_x)\mu_v + \frac{1}{4} b_1(w + \omega_y)\mu_v$	$-\frac{1}{4} a_0 b_1 \mu_v^2$
cos ψ	$-b_1 - (w + \omega_y)$	$a_0\mu_v$	$\frac{1}{2}\left(a_0 - \frac{1}{2} b_1\right)\mu_v^2$		$-\frac{1}{4} a_1(w + \omega_y)\mu_v + \frac{1}{4} b_1(y - \omega_x)\mu_v + b_1\lambda_v$	$\frac{1}{4} a_0 a_1 \mu_v^2$

(88d)

Rotor Torque

The effects of tip stall at the higher values of μ_v and C_T/σ_3 on C_Q are large and may be approximately evaluated for high-speed flight where λ_v is negative, as follows: The retreating blade will be stalled outboard of the nondimensional radius (for λ_v negative)

$$x_s = \frac{\lambda_v + \mu_v \tan\left(\frac{c_{l_{max}}}{a} - A_0 - a_1 - \Delta\theta_t\right)}{y + \tan\left(\frac{c_{l_{max}}}{a} - A_0 - a_1 - \Delta\theta_t\right)} \tag{89a}$$

where $\Delta\theta_t$ is the aerodynamic blade twist between the reference station and the tip. Assuming a jump of 0.08 in the value of c_{d_0} at the stall and that the rotor area within which blade stall exists is a segment of minimum radius x_s and symmetric about $\psi = 3\pi/2$, the increment ΔC_{Q_s} to C_Q due to tip stall is approximately

$$\Delta C_{Q_s} \approx \frac{b\sigma_4}{6\pi}(1 - \mu_v)^2(1 - x_s)\sqrt{1 - x_s^2} \tag{89b}$$

(If $x_s < \mu_v$ or $x_s > 1$ equation (89b) is not applicable and $\Delta C_{Q_s} = 0.$) Then

$$\frac{2C_Q}{b} = -(\text{Constant terms of } C_{xy} \text{ with subscripts } n \text{ on } \sigma_n,\ I_{nc},\ \text{and } I_{ns} \text{ increased to } n + 1) + \frac{2\Delta C_{Q_s}}{b} \tag{90a}$$

For steady-state calculations equation (90a) may be reduced to

$$\frac{2C_Q}{b} = \frac{2C_T\left(\frac{1}{2}y\mu_v - \lambda_v\right)}{b(1 - \mu_v^2)} + \frac{2\Delta C_{Q_s}}{b} +$$

$$\epsilon_0\left[\left(1 + \frac{1}{4}w^2\right)\sigma_4 - \frac{1}{2}a_0 w\mu_v\sigma_3 + \frac{1}{2}\left(\lambda_v^2 + \mu_v^2\right)\sigma_2\right] +$$

$$\epsilon_1\left[I_{4c} + \frac{1}{2}a_0 b_1\mu_v I_{3c} + \frac{1}{2}\left(\mu_v + a_1\lambda_v\right)\mu_v I_{2c} + \left(a_1\mu_v - \lambda_v\right)I_{3s}\right] +$$

$$\epsilon_2\left[\left(a_1\mu_v - \lambda_v\right)I_{3c} - \left(1 - \frac{1}{2}b_1 w\right)I_{4s} - \frac{1}{2}a_0 b_1\mu_v I_{3s} -\right.$$

$$\left.\frac{1}{2}\left(a_1\lambda_v + \mu_v\right)\mu_v I_{2s}\right] \qquad (90b)$$

Rotor X Force

The value of the rotor X-force coefficient C_X is

$$\frac{2C_X}{b} = -\left(\text{Sine terms of } C_{xy}\right) \qquad (91)$$

However, the greater part of C_X arising from the lateral variation in blade circulation is a small difference between large quantities which are principally functions of a_1 and A_0. It follows that this part of C_X is more accurately obtained from the circulation equations than from the blade-element equations. Thus for steady-state solutions

$$\frac{2C_X}{b} \approx \frac{2C_T(2\lambda_v\mu_v - y)}{b(1 - \mu_v^2)} + \epsilon_0(2\mu_v + y\lambda_v)\sigma_2 +$$

$$\epsilon_1\left[(a_1\lambda_v + 2\mu_v)I_{2c} + (a_1 - y)I_{3s} + \left(\frac{3}{4}a_1\mu_v - \lambda_v\right)\mu_v I_{1s}\right] +$$

$$\epsilon_2\left[(a_1 - y)I_{3c} + \left(\frac{3}{4}a_1\mu_v - \lambda_v\right)\mu_v I_{1c} - (2\mu_v + a_1\lambda_v)I_{2s}\right] \qquad (92)$$

Rotor Y Force

The value of the rotor Y-force coefficient is

$$\frac{2C_Y}{b} = \text{Cosine terms of } C_{xy} \qquad (93)$$

As in the expression for C_x the above value of C_y given by the blade-element equation is a small difference between large quantities and the result for steady-state flight is more accurately obtained from the circulation expression

$$C_y \approx \frac{C_T\left(w - \frac{3}{2} a_0 \mu_v\right)}{1 - \mu_v^2} \tag{94}$$

Second-Harmonic Flapping

Again letting k_{a_0} be the spring constant relating the blade-root bending moment in foot-pounds to the angular deflection in radians of the three-quarter-radius point of the blades from the unstressed position, it follows that the magnitude of the cosine component of the second harmonic of the blade flapping angle is

$$a_2 \approx \frac{J + KL}{1 - KM} \tag{95}$$

Similarly the magnitude of the sine component is

$$b_2 \approx \frac{L + JM}{1 - KM} \tag{96}$$

where

J $\left(\text{terms not involving } b_2 \text{ in the } \cos 2\psi \text{ row of thrust equation (53) with the I factors changed to one higher subscript}\right) \times \left(\frac{\frac{1}{2}\rho\pi\Omega^2 R^5 a}{3I_1\Omega^2 - k_{a_0}}\right)$

K $\left(\text{coefficients of } b_2 \text{ in the } \cos 2\psi \text{ row of thrust equation (53) with the I factors changed to one higher subscript}\right) \times \left(\frac{\frac{1}{2}\rho\pi\Omega^2 R^5 a}{3I_1\Omega^2 - k_{a_0}}\right)$

L $\left(\text{terms not involving } a_2 \text{ in the } \sin 2\psi \text{ row of thrust equation (53) with the I factors changed to one higher subscript}\right) \times \left(\frac{\frac{1}{2}\rho\pi\Omega^2 R^5 a}{3I_1\Omega^2 - k_{a_0}}\right)$

M (coefficients of a_2 in the sin 2ψ row of thrust equation (53) with the I factors changed to one higher subscript) $\times \left(\frac{\frac{1}{2}\rho\pi\Omega^2R^5a}{3I_1\Omega^2 - k_{a_0}}\right)$ -

For steady-state flight conditions where $\omega_x = \omega_y = 0$ the expressions for the factors J, K, L, and M may be simplified to

$$J \approx \frac{\frac{1}{2}\rho\pi a\Omega^2R^5}{3I_1\Omega^2 - k_{a_0}}\left[-\frac{1}{2}\left(a_1\lambda_v + \mu_v\right)\mu_v I_{2c} - \left(a_1 - \frac{1}{2}y\right)\mu_v I_{3s}\right] \tag{97}$$

$$K \approx \frac{\frac{1}{2}\rho\pi a\Omega^2R^5}{3I_1\Omega^2 - k_{a_0}}\left(-2I_{4s}\right) \tag{98}$$

$$L \approx \frac{\frac{1}{2}\rho\pi a\Omega^2R^5}{3I_1\Omega^2 - k_{a_0}}\left[-\frac{1}{2}b_1\lambda_v\mu_v I_{2c} - \left(b_1 + \frac{1}{2}w\right)\mu_v I_{3s} + \frac{1}{2}a_0\mu_v{}^2 I_{2s}\right] \tag{99}$$

$$M \approx \frac{\frac{1}{2}\rho\pi a\Omega^2R^5}{3I_1\Omega^2 - k_{a_0}}\left(2I_{4s}\right) \tag{100}$$

and I_1 is the mass moment of inertia of the blade about the flapping hinge.

It may be noted that $k_{a_0} = 0$ for blades having a flapping hinge at the axis of rotation. If the flapping hinge is located at radius r_β, then

$$k_{a_0} \approx \frac{r_\beta\bar{r}M_B\Omega^2}{1 - \frac{r_\beta}{0.75R}}$$

Amplitude of Constant and First-Harmonic Components of Lag Angles in Unaccelerated Flight

For an articulated rotor having lag hinges normal to the plane of rotation and located at a small radius e the equilibrium blade lag angle E_0 is

$$E_0 \approx \frac{\frac{1}{2}\rho\pi R^5}{M_\zeta e\left(1 - \frac{e}{0.7R}\right)}\left[-\frac{2C_Q}{b} \text{ from equation (90)}\right] \tag{101}$$

where M_ζ is the mass moment of the blade about the lag hinge.

Similarly the coefficients of the cosine and sine components of the lag angle are

$$E_1 \approx \frac{\frac{1}{2}\rho\pi R^5 E_\zeta - 2a_0 b_{1s} I_\zeta}{M_\zeta e - I_\zeta} \tag{102}$$

and

$$F_1 \approx \frac{\frac{1}{2}\rho\pi R^5 F_\zeta + 2a_0 a_{1s} I_\zeta}{M_\zeta e - I_\zeta} \tag{103}$$

where a_{1s} and b_{1s} are the $\cos\psi$ and $\sin\psi$ components of the angle between the tip-path plane and the hub plane. For unaccelerated flight the values of a_{1s} and b_{1s} are approximately

$$a_{1s} \approx \alpha_v - \alpha_f \tag{104}$$

$$b_{1s} \approx \theta_{xf} - \theta_x \tag{105}$$

where θ_{xf} is the equilibrium lateral tilt of the fuselage.

Also

I_ζ mass moment of inertia of a blade about lag hinge

E_ζ coefficient of $\cos\psi$ in equation (88) for C_{xy} with subscripts of I factors changed from n to n + 1; approximate value from circulation equations is

$$E_\zeta = \frac{2C_T\left(\frac{3}{4}w - a_0\mu_v\right)}{b\left(1 - \mu_v^2\right)} \tag{106}$$

F_ζ coefficient of $\sin\psi$ in equation (88) for C_{xy} with subscripts of I factors changed from n to n + 1; approximate value from circulation equations is

$$F_\zeta = \frac{2C_T\left(\frac{3}{4}y - \frac{4}{3}\lambda_v\mu_v\right)}{b(1 - \mu_v^2)} - 0.008(2\mu_v + y\lambda_v)\sigma_3 + \frac{0.085C_T^2\mu_v\sigma_4}{b^2\sigma_3^2(1 - \mu_v^2)^2} \tag{107}$$

Thrust Unbalance

Two-bladed rotor.- The second-harmonic variation in C_T for a two-bladed rotor is

$$\frac{\Delta C_T}{a} = \text{Fourth + fifth rows of equation (53)} \tag{108}$$

For $\omega_x = \omega_y = 0$ and steady-state conditions, the equation for the amplitude may be simplified to

$$\frac{\Delta C_T}{a} \approx \left\{\left[2a_2I_{3s} - \left(b_1 + \frac{1}{2}w\right)\mu_vI_{2s} + \frac{1}{2}a_0\mu_v^2I_{1s}\right]^2 + \left(2b_2I_{3s} + a_1\mu_vI_{2s}\right)^2\right\}^{1/2} \tag{109}$$

Three-bladed rotor.- The third-harmonic variation in C_T for a three-bladed rotor is approximately

$$\frac{2\Delta C_T}{3a} \approx \text{Sixth + seventh rows of equation (53)} \tag{110}$$

or for $\omega_x = \omega_y = 0$ the amplitude is approximately

$$\frac{2\Delta C_T}{3a} \approx -\frac{1}{4}\left(a_1^2 + b_1^2\right)^{1/2} \mu_v^2 I_{1s} \tag{111}$$

An Independence-of-Blade-Element Analysis for Hovering, Vertical Ascent, and Convertaplane Propeller Condition

The use of the relation $c_l = a \sin \alpha$ permits a considerable simplification of the equations resulting from the assumption of the independence of blade elements. As the exact propeller solutions of Betz, Goldstein, and Theodorsen are not applicable to a lifting rotor at zero or small advance ratios, a simple analysis of the independence of blade elements may be useful.

From momentum considerations the thrust dT on an annulus of the rotor disk $2\pi r\, dr$ is related to the induced velocity V_i at the rotor element by the expression

$$\frac{dT}{4\pi\rho r\, dr} = V_i\left(V_i + V \sin \alpha_v\right) \tag{112}$$

But

$$V_i + V \sin \alpha_v = U \sin \phi_v \tag{113}$$

Thus

$$\frac{dT}{4\pi\rho r\, dr} = \left(U \sin \phi_v\right)\left(U \sin \phi_v - V \sin \alpha_v\right) \tag{114}$$

The thrust of the annulus is also equal to the thrust acting on the portions of the blades within the annulus which is

$$dT = \frac{1}{2} \rho b U^2 c c_l \cos \phi_v \, dr \tag{115}$$

where

$$c_l = a \sin \alpha_r = a\left(\sin \theta_v \cos \phi_v + \cos \theta_v \sin \phi_v\right) \tag{116}$$

Thus

$$dT = \frac{1}{2} \rho ab\left(U \cos \phi_v\right)\left[\sin \theta_v\left(U \cos \phi_v\right) + \cos \theta_v\left(U \sin \phi_v\right)\right] c \, dr \tag{117}$$

Substituting the above values of dT in equation (114) and solving for $U \sin \phi_v$

$$\frac{U \sin \phi_v}{\Omega R} = \left(\frac{v_a}{2} + \frac{ab\sigma_r}{16} \cos \theta_v\right) - \sqrt{\left(\frac{v_a}{2} + \frac{ab\sigma_r}{16} \cos \theta_v\right)^2 + \frac{ab\sigma_r}{8} x \sin \theta_v} \tag{118}$$

where

$$v_a = \frac{V \sin \alpha_v}{\Omega R} \tag{119}$$

$$\sigma_r = \frac{c}{\pi R} \tag{120}$$

Then from equation (117)

$$\frac{2C_T}{ab} = \int_{x_1}^{1} \left[x \sin \theta_v + \left(\frac{U \sin \phi_v}{\Omega R}\right) \cos \theta_v\right] \sigma_r x \, dx \tag{121}$$

where the value of $\frac{U \sin \phi_v}{\Omega R}$ at x is given by equation (118). Similarly, from blade-element considerations

$$\frac{2C_Q}{b} = -a \int_{x_1}^{1} \left(\frac{U \sin \phi_v}{\Omega R}\right)\left[x \sin \theta_v + \left(\frac{U \sin \phi_v}{\Omega R}\right) \cos \theta_v\right] \sigma_r x \, dx +$$

$$\int_{x_1}^{1} \frac{c_{d_o}}{\sin \alpha_r} \left[x \sin \theta_v + \left(\frac{U \sin \phi_v}{\Omega R}\right) \cos \theta_v\right] \sigma_r x^2 \, dx \qquad (122)$$

where the values of $\frac{c_{d_o}}{\sin \alpha_r}$ are obtained from a plot of $\frac{c_{d_o}}{\sin \alpha_r}$ against α_r for the blade airfoil at values of α_r given by the relation

$$\alpha_r = \theta_v + \tan^{-1}\left[\frac{1}{x}\left(\frac{U \sin \phi_v}{\Omega R}\right)\right] \qquad (123)$$

If it is necessary to take into account the rotation of the slipstream for large rates of vertical ascent or the propeller condition, this may be accomplished to a first approximation by using an effective Ω, Ω_e, in every case where

$$\Omega_e = \Omega\left(1 - \frac{1}{4} C_T\right) \qquad (124)$$

The geometry of the above equations is exact and they are convenient for graphical or numerical integration on account of the repetition of factors.

Neglecting the induced radial and tangential velocity components, the optimum blade-angle distribution for minimum induced power and a given blade-chord distribution and nondimensional axial flight-path velocity v_a may be obtained by setting $\frac{U \sin \phi_v}{\Omega R}$ equal to the constant value λ_v giving

$$\sin \theta_v = \frac{\lambda_v(\lambda_v - v_a)x}{k(\lambda_v^2 + x^2)} \left\{ 1 + \sqrt{1 + \frac{(\lambda_v^2 + x^2)\left[k^2 - (\lambda_v - v_a)^2\right]}{(\lambda_v - v_a)^2 x^2}} \right\} \tag{125}$$

where

$$k = \frac{ab\sigma_r}{8} \tag{126}$$

and

$$\lambda_v = \frac{v_a}{2} - \sqrt{\left(\frac{v_a}{2}\right)^2 + \frac{1}{2} C_T} \tag{127}$$

The optimum chord distribution for a given desired constant value of c_l along the blade and the same restrictions is

$$\sigma_r = \frac{8\lambda_v(\lambda_v - v_a)}{bc_l\sqrt{\lambda_v^2 + x^2}} \tag{128}$$

For this optimum chord distribution, the optimum distribution of θ_v reduces to

$$\sin \theta_v = \frac{xc_l}{a\sqrt{\lambda_v^2 + x^2}} \left[1 + \sqrt{1 + \frac{a^2\lambda_v^2 - c_l^2(\lambda_v^2 + x^2)}{c_l^2 x^2}} \right] \tag{129}$$

For calculations where the flight-path velocity and equilibrium value of C_T are known or can be estimated, the following procedure may be followed:

(1) Calculate and plot the radial distribution of σ_r

(2) Calculate the effective value of C_T and v_a where

$$C_{T_e} = C_T\left(\frac{\Omega}{\Omega_e}\right)^2$$

$$v_{a_e} = v_a\left(\frac{\Omega}{\Omega_e}\right)$$

(3) Calculate the approximate value of A_0 from equation (72) which for these flight conditions reduces to

$$\sin A_0 \approx \frac{\left(\frac{2C_{T_e}}{ab} - \sigma_{3s} - \lambda_v\sigma_{2c}\right)}{\left(\sigma_{3c} - \lambda_v\sigma_{2s}\right)}$$

(4) Calculate and plot the radial distribution of $\theta_v = A_0 + \theta_t$ for the value of A_0 obtained under item (3) and two lower values at increments of several degrees

(5) Calculate and plot the radial distribution of $U \sin \phi_v/\Omega_e R$ for the above distribution of θ_v from equation (118) using $\Omega = \Omega_e$ throughout

(6) Calculate and plot the radial distribution of the integrand of equation (121) for the three values of A_0 and graphically or numerically integrate for the values of $2C_{T_e}/ab$ corresponding to the three values of A_0

(7) Obtain the correct value of A_0 from a plot of C_{T_e} against A_0

(8) Calculate and plot the radial distribution of the integrand of equation (122) for the three values of A_0 and graphically or numerically integrate for the values of $2C_{Q_e}/b$ corresponding to the three values of A_0

(9) Obtain the equilibrium value of C_{Q_e} at the equilibrium value of A_0 from a plot of C_{Q_e} against A_0

(10) Calculate the equilibrium value of $C_Q = C_{Q_e}\left(\frac{\Omega_e}{\Omega}\right)^2$

Comparison of Experimental and Calculated Values of Parameters

Table 6 shows a comparison of the experimental data of reference 2 for those runs where $C_T \approx 0.00545$ with the values calculated by the approximate blade-element equations of this report. The blade-element lift-curve slope was assumed by the authors to have been $a = 6.5$ from the experimental results of reference 6. The values of ϵ_0, ϵ_1,

and ϵ_2 were evaluated for the points c_{d_o} = 0.0090, 0.0105, and 0.0170 at c_l = 0, 0.5, and 1.0, respectively, from figure 19 of reference 6.

The exact solutions for the various parameters differ from the tabulated approximate solutions by a negligible amount for these helicopter flight conditions.

A consideration of the results presented in table 6 would indicate that much of the remaining discrepancy between experimental and calculated blade angles and torque coefficients may be due to the neglect, in the present calculations, of the effects of the rotor induced velocity on the lift and drag of the fuselage.

It may be noted that the longitudinal component of the angle $\tan^{-1}\left(\frac{C_X}{2C_T}\right)$ between the rotor resultant force and the thrust component normal to the tip-path plane is very small for all these helicopter flight conditions and that the direction of the resultant is inclined forward for those flight conditions where there is a net downflow through the rotor. The inclinations of the tip-path plane to the horizontal θ_x and θ_y are also small angles and, consequently, for many unaccelerated-flight helicopter calculations the rotor resultant force can be assumed to be perpendicular to the tip-path plane and the thrust equal to the gross weight without introducing serious errors.

CONCLUDING DISCUSSION

Simple relations for the rotor blade angles and the values of C_Q, C_X, and C_Y, derived upon the assumption of a triangular distribution of blade-element circulation along the radius and a sinusoidal variation with azimuth angle in conjunction with a linear variation of profile drag with lift, would appear to be useful for helicopter and convertaplane performance estimation and the determination of the equilibrium angle of attack and lateral tilt of the tip-path plane.

The blade-element equations, based upon the relation that $c_l = a \sin \alpha_r = a(\sin \theta_v \cos \phi_v + \cos \theta_v \sin \phi_v)$, and the σ_{nc} and σ_{ns} functions of the blade-chord and blade-twist distribution afford a reasonably exact and concise treatment of the geometry and should be useful for convertaplane as well as helicopter calculations.

The use of the empirical relation $c_{d_o} = \epsilon_0 + \epsilon_1 \sin \alpha_r + \epsilon_2 \cos \alpha_r$, rather than the usual expression that $c_{d_o} = \delta_0 + \delta_1 \alpha_r + \delta_2 \alpha_r^2$, considerably simplifies the equations for the in-plane forces and moments and presents a sufficiently exact solution of the geometry for helicopter calculations.

For convertaplane calculations, the approximation that $c_{d_o} = \epsilon_1 \sin \alpha_r + \epsilon_2 \cos \alpha_r$ allows an exact treatment of the geometry and should be a sufficiently accurate expression for c_{d_o} at the larger advance ratios where the effects of the profile drag become of less relative importance.

The larger sources of the remaining errors in the blade-element analysis probably have the following order of importance for contemporary helicopters:

(1) The neglect of the effects of blade-element stall implied in the relation that $c_l = a \sin \alpha_r$

(2) The neglect of the effects of blade flexibility

(3) The neglect of the radial variation in the normal component of the induced velocity

(4) The neglect of the effects of compressibility on the tip sections of the advancing blade.

Georgia Institute of Technology
Atlanta, Ga., May 15, 1951

REFERENCES

1. Drees, Meijer, Jr.: A Theory of Airflow through Rotors and Its Application to Some Helicopter Problems. The Jour. Helicopter Assoc. (Great Britain), vol. 3, no. 2, July-Aug.-Sept. 1949, pp. 79-104.

2. Myers, Garry C., Jr.: Flight Measurements of Helicopter Blade Motion with a Comparison between Theoretical and Experimental Results. NACA TN 1266, 1947.

3. Castles, Walter, Jr., and Gray, Robin B.: Empirical Relation between Induced Velocity, Thrust, and Rate of Descent of a Helicopter Rotor as Determined by Wind-Tunnel Tests on Four Model Rotors. NACA TN 2474, 1951.

4. Glauert, H.: Airplane Propellers. The Blade Element Theory. Vol. IV of Aerodynamic Theory, div. L, ch. V, sec. 9, W. F. Durand, ed., Julius Springer (Berlin), 1935, pp. 229-230.

5. Young, A. D., and Winterbottom, N. E.: Note on the Effect of Compressibility on the Profile Drag of Aerofoils at Subsonic Mach Numbers in the Absence of Shock Waves. R. & M. No. 2400, British A.R.C., 1940.

6. Tetervin, Neal: Airfoil Section Data From Tests of 10 Practical-Construction Sections of Helicopter Rotor Blades Submitted by the Sikorsky Aircraft Division, United Aircraft Corporation. NACA MR, Sept. 1944.

7. Gessow, Alfred, and Meyers, Garry C., Jr.: Flight Tests of a Helicopter in Autorotation, Including a Comparison with Theory. NACA TN 1267, 1947.

TABLE 1

VALUES OF σ_n FOR BLADES WITH LINEAR TAPER

[Interpolate for values for given t; $\sigma_0 = \frac{c_o}{\pi R}$;

$t = \frac{c_{tip}}{c_o} - 1$; $c = c_o(1 + tx)$]

t	σ_1/σ_0	σ_2/σ_0	σ_3/σ_0	σ_4/σ_0
$x_1 = 0.15$				
0	0.8500	0.4888	0.3322	0.2499
-1	.3612	.1566	.0823	.0499
$x_1 = 0.20$				
0	0.8000	0.4800	0.3307	0.2496
-1	.3200	.1493	.0811	.0497

TABLE 2

VALUES OF σ_{nc} FOR BLADES WITH LINEAR TAPER, LINEAR TWIST, AND $x_1 = 0.15$

[Interpolate for values for given t first and then for values for given θ_1; reference station for A_0 at $x = 0$; $\sigma_0 = \frac{c_o}{\pi R}$; $t = \frac{c_{tip}}{c_o} - 1$; $c = c_o(1 + tx)$; $\theta_t = \theta_1 x$]

θ_1 (deg)	σ_{1c}/σ_0		σ_{2c}/σ_0		σ_{3c}/σ_0		σ_{4c}/σ_0	
	t = 0	t = -1	t = 0	t = -1	t = 0	t = -1	t = 0	t = -1
0	0.8500	0.3612	0.4888	0.1566	0.3322	0.0823	0.2499	0.0499
-4	.8492	.3611	.4882	.1565	.3317	.0822	.2495	.0498
-8	.8468	.3604	.4864	.1561	.3303	.0820	.2483	.0497
-12	.8427	.3594	.4833	.1555	.3278	.0816	.2462	.0494
-16	.8371	.3580	.4791	.1546	.3244	.0810	.2434	.0490
-20	.8299	.3562	.4737	.1536	.3201	.0803	.2398	.0485
-24	.8211	.3541	.4671	.1522	.3148	.0794	.2354	.0478
-28	.8108	.3515	.4594	.1507	.3087	.0784	.2303	.0471

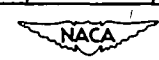

TABLE 3

VALUES OF σ_{ns} FOR BLADES WITH LINEAR TAPER, LINEAR TWIST, AND $x_1 = 0.15$

[Interpolate for values for given t first and then for values for given θ_1; reference station for A_0 at $x = 0$; $\sigma_0 = \frac{c_o}{\pi R}$; $t = \frac{c_{tip}}{c_o} - 1$; $c = c_o(1 + tx)$; $\theta_t = \theta_1 x$]

θ_1 (deg)	σ_{1s}/σ_0		σ_{2s}/σ_0		σ_{3s}/σ_0		σ_{4s}/σ_0	
	t = 0	t = -1	t = 0	t = -1	t = 0	t = -1	t = 0	t = -1
0	0	0	0	0	0	0	0	0
-4	-.0341	-.0109	-.0232	-.0057	-.0174	-.0035	-.0139	-.0023
-8	-.0681	-.0219	-.0463	-.0115	-.0348	-.0070	-.0279	-.0047
-12	-.1020	-.0327	-.0693	-.0172	-.0521	-.0104	-.0417	-.0070
-16	-.1356	-.0435	-.0920	-.0229	-.0692	-.0138	-.0553	-.0092
-20	-.1699	-.0531	-.1145	-.0284	-.0860	-.0173	-.0688	-.0115
-24	-.2017	-.0650	-.1367	-.0341	-.1026	-.0206	-.0820	-.0137
-28	-.2340	-.0756	-.1585	-.0396	-.1189	-.0239	-.0950	-.0159

TABLE 4

VALUES OF σ_{nc} FOR BLADES WITH LINEAR TAPER, HELICAL TWIST, AND $x_1 = 0.20$

[Interpolate for values for given t first and then for values of given θ_T; reference station for A_0 at blade tip; $\sigma_0 = \frac{c_0}{\pi R}$; $t = \frac{c_{tip}}{c} - 1$; $c = c_0(1 + tx)$; $\theta_t = \tan^{-1}\left(\frac{1}{x} \tan \theta_T\right)$]

θ_T (deg)	σ_{1c}/σ_0		σ_{2c}/σ_0		σ_{3c}/σ_0		σ_{4c}/σ_0	
	t = 0	t = -1	t = 0	t = -1	t = 0	t = -1	t = 0	t = -1
0	0.8000	0.3200	0.4800	0.1493	0.3307	0.0810	0.2496	0.0497
-4	.7906	.3144	.4762	.1474	.3287	.0803	.2484	.0493
-8	.7654	.3002	.4651	.1419	.3233	.0782	.2451	.0483
-12	.7305	.2804	.4500	.1351	.3149	.0751	.2398	.0468
-16	.6907	.2594	.4313	.1270	.3042	.0714	.2328	.0448
-20	.6489	.2385	.4104	.1185	.2919	.0674	.2244	.0427
-24	.6065	.2184	.3882	.1100	.2782	.0632	.2151	.0404
-28	.5645	.1994	.3651	.1016	.2635	.0590	.2046	.0379
-32	.5231	.1815	.3416	.0934	.2481	.0547	.1935	.0354

TABLE 5

VALUES OF σ_{ns} FOR BLADES WITH LINEAR TAPER, HELICAL TWIST, AND $x_1 = 0.20$

[Interpolate for values for given t first and then for values for given θ_T; reference station for A_0 at blade tip; $\sigma_0 = \frac{c_0}{\pi R}$; $t = \frac{c_{tip}}{c_0} - 1$; $c = c_0(1 + tx)$; $\theta_t = \tan^{-1}\left(\frac{1}{x} \tan \theta_T\right)$]

θ_T (deg)	σ_{1s}/σ_0		σ_{2s}/σ_0		σ_{3s}/σ_0		σ_{4s}/σ_0	
	t = 0	t = -1	t = 0	t = -1	t = 0	t = -1	t = 0	t = -1
0	0	0	0	0	0	0	0	0
-4	-.1106	-.0553	-.0553	-.0220	-.0333	-.0103	-.0230	-.0056
-8	-.2121	-.1045	-.1076	-.0422	-.0654	-.0200	-.0454	-.0110
-12	-.3005	-.1452	-.1553	-.0596	-.0957	-.0287	-.0669	-.0160
-16	-.3761	-.1780	-.1981	-.0744	-.1237	-.0364	-.0872	-.0205
-20	-.4405	-.2044	-.2365	-.0872	-.1494	-.0431	-.1062	-.0245
-24	-.4956	-.2256	-.2701	-.0972	-.1728	-.0490	-.1239	-.0281
-28	-.5430	-.2428	-.3002	-.1060	-.1941	-.0540	-.1401	-.0313
-32	-.5838	-.2570	-.3269	-.1134	-.2134	-.0584	-.1551	-.0342

TABLE 6

COMPARISON OF EXPERIMENTAL AND CALCULATED VALUES OF PARAMETERS FOR THOSE RUNS OF REFERENCE 1 FOR WHICH $C_T \approx 0.00545$

[All angles in deg; tip stall on run 2]

Parameter	Run 7 $C_T = 0.00545$; $\Omega R = 443$ ft/sec Level flight at 43.7 mph			Run 4 $C_T = 0.00538$; $\Omega R = 447$ ft/sec Level flight at 58.6 mph			Run 2 $C_T = 0.00545$; $\Omega R = 445$ ft/sec Level flight at 71.7 mph		
	Experimental	Calculated (a)	Calculated (b)	Experimental	Calculated (a)	Calculated (b)	Experimental	Calculated (a)	Calculated (b)
α_r	-2.2			-4.5			-6.9		
α_f	23.4			23.7			24.1		
ϕ_c	0			0			0		
a_v	-2.08	-1.99		-3.83	-3.75		-5.82	-5.75	
A_0	7.11	7.14	7.35	8.17	7.65	7.95	10.10	72	9.19
a_1	2.92	3.08	2.86	4.37	4.41	3.84	6.08	6.65	5.05
a_0	8.16	8.28	7.99	8.30	8.25	8.02	8.67	8.39	8.21
b_1	3.24	2.74	2.78	3.30	3.01	3.06	3.93	3.39	3.40
a_2	0.24	0.16	0.17	0.35	0.28	0.28	0.46	0.43	0.42
b_2	0.00	0.00	-0.04	-0.08	0.00	-0.09	-0.11	0.00	-0.17
C_Q	0.000202	0.000204	0.000205	0.000244	0.000230	0.000218	0.000342	[d]0.000354	[d]0.000328
E_0	-7.45	-7.68	-7.73	-8.83	-8.63	-8.18	-12.50	-13.32	-12.36
[e]E_1	0.41	0.52		0.54	0.57		0.67	0.66	
[e]F_1	-0.21	-0.08		-0.18	-0.11		-0.87	-0.18	
C_x		-0.000041	-0.000046		-0.000056	-0.000062		-0.000092	-0.000110
C_y		-0.000283			-0.000319			-0.000370	
$\text{Tan}^{-1}\left(\frac{C_x}{2C_T}\right)$		-0.21			-0.30			-0.48	
θ_x		-0.08			-0.09			0.06	
θ_y	-2.08	-1.99		-3.83	-3.74		-5.82	-5.75	
$\left(\frac{\Delta C_T}{C_T}\right)_{3rd}$		0.013			0.029			0.058	

[a]Calculated from circulation equations.

[b]Calculated from blade-element equations.

[c]3 sq ft added to fuselage drag area f from reference 7 to allow for rotor-hub, blade-shank, counter-torque-rotor, and engine-cooling drag.

[d]Includes correction for tip stall.

[e]Mechanical input subtracted.

NACA

TABLE 6 - Concluded

COMPARISON OF EXPERIMENTAL AND CALCULATED VALUES OF PARAMETERS FOR THOSE RUNS OF REFERENCE 1 FOR WHICH $C_T \approx 0.00545$ - Concluded

Parameter	Run 11 $C_T = 0.00546$; $\Omega R = 443$ ft/sec 525 ft/min climb at 51.8 mph			Run 15 $C_T = 0.00549$; $\Omega R = 443$ ft/sec 1260 ft/min autorotative descent at 37.7 mph		
	Experimental	Calculated (a)	Calculated (b)	Experimental	Calculated (a)	Calculated (b)
α_f	-10.1			-19.4		
^cf	25.4			26.4		
ϕ_c	-6.51			20.80		
α_v	-9.97	-9.55		18.77	18.55	
A_0	10.00	8.95	9.50	3.40	4.10	3.71
a_1	4.23	4.32	3.81	1.07	1.84	1.80
a_0	9.15	8.38	8.42	7.55	8.40	7.80
b_1	3.56	2.78	2.88	2.86	2.62	2.85
a_2	0.33	0.22	0.24	0.08	0.11	0.12
b_2	-0.10	0.00	-0.08	-0.02	0.00	-0.00
C_Q	0.000359	0.000328	0.000322	-0.000008	-0.000014	-0.000016
E_0	-13.03	-12.36	-12.14	-0.03	0.51	0.62
$^eE_1$	0.70	0.55		0.21	0.53	
$^eF_1$	-0.37	-0.16		0.26	-0.01	
C_x		-0.000086	-0.000095		0.000011	0.000010
C_y		-0.000296			-0.000293	
$\text{Tan}^{-1}\left(\frac{C_x}{2C_T}\right)$		-0.45			0.06	
θ_x		0.71			1.63	
θ_y	-3.40	-2.98		2.03	2.24	
$\left(\frac{\Delta C_T}{C_T}\right)_{3rd}$		0.021			0.008	

[a]Calculated from circulation equations.

[b]Calculated from blade-element equations.

[c]3 sq ft added to fuselage drag area f from reference 7 to allow for rotor-hub, blade-shank, counter-torque-rotor, and engine-cooling drag.

[e]Mechanical input subtracted.

TABLE 7

VALUES OF $\lambda_i = \frac{v}{\Omega R}\sqrt{\frac{2 - 3\mu_v^2}{C_T}}$ FOR GIVEN VALUES OF $\lambda_x = \mu_v\sqrt{\frac{2 - 3\mu_v^2}{C_T}}$

AND $\lambda_z = \frac{V \sin \alpha_v}{\Omega R}\sqrt{\frac{2 - 3\mu_v^2}{C_T}}$

λ_z	λ_x									
	0	0.40	0.60	0.80	1.00	1.20	1.40	1.60	1.80	2.00
2.40	[a]0.960	[b]0.740	[b]0.580	0.481	0.457	0.433	0.410	0.390	0.371	0.349
2.20	[a]1.14	[b].88	[b].68	.543	.509	.476	.444	.418	.392	.369
2.00	[a]1.36	[b]1.07	[b].82	.630	.574	.526	.484	.450	.418	.389
1.80	[a]1.65	[b]1.34	[b]1.03	.767	.659	.585	.529	.483	.445	.410
1.60	[a]2.26	[b]1.81	[b]1.42	1.000	.769	.654	.577	.518	.472	.432
1.40	[a]2.44	[b]2.05	[b]1.77	1.220	.896	.727	.627	.550	.496	.452
1.20	[a]2.24	[b]1.88	[b]1.65	1.25	.976	.789	.668	.582	.520	.470
1.00	[a]2.01	[b]1.72	[b]1.52	1.21	1.000	.824	.698	.613	.539	.485
.80	[a]1.80	[b]1.56	[b]1.39	1.15	.984	.833	.713	.621	.552	.494
.60	[a]1.60	[b]1.41	[b]1.27	1.07	.947	.820	.712	.625	.556	.500
.40	[a]1.42	[b]1.28	[b]1.16	1.00	.897	.792	.698	.619	.554	.500
.20	[a]1.25	[b]1.15	[b]1.06	.924	.842	.756	.677	.606	.547	.494
0	[a]1.10	[b]1.02	[b].96							
0	1.000	.961	.914	.854	.786	.715	.648	.586	.533	.486
-.20	.905	.874	.833	.787	.731	.673	.613	.564	.516	.474
-.40	.820	.796	.765	.724	.680	.632	.584	.539	.497	.461
-.60	.744	.725	.699	.668	.630	.592	.551	.513	.477	.443
-.80	.677	.658	.640	.615	.586	.553	.520	.487	.453	.426
-1.00	.618	.605	.588	.569	.544	.517	.489	.462	.435	.409
-1.20	.566	.556	.543	.526	.506	.484	.460	.433	.413	.392
-1.40	.521	.512	.501	.488	.472	.453	.433	.413	.394	.374
-1.60	.481	.473	.464	.454	.440	.426	.408	.391	.374	.358
-1.80	.445	.439	.432	.424	.411	.399	.385	.371	.356	.341
-2.00	.414	.409	.403	.395	.386	.376	.364	.352	.339	.326
-2.40	.362	.358	.355	.350	.342	.334	.327	.318	.308	.298
-2.80	.320	.318	.316	.311	.306	.301	.294	.287	.280	.273
-3.20	.287	.284	.282	.280	.276	.272	.267	.262	.256	.250
-3.60	.259	.257	.256	.254	.251	.248	.244	.240	.236	.231
-4.00	.236	.235	.234	.233	.230	.227	.225	.223	.221	.214
-5.00	.193	.192	.192	.191	.189	.187	.186	.184	.182	.180
-6.00	.162	.162	.162	.161	.160	.159	.158	.157	.156	.155
-8.00	.123	.123	.123	.122	.122	.122	.121	.121	.120	.120
-10.00	.100	.100	.100	.100	.099	.099	.099	.098	.098	.097

[a]Experimental.

[b]Estimated.

TABLE 7 - Concluded

VALUES OF $\lambda_i = \frac{v}{\Omega R}\sqrt{\frac{2 - 3\mu_v^2}{C_T}}$ FOR GIVEN VALUES OF $\lambda_x = \mu_v\sqrt{\frac{2 - 3\mu_v^2}{C_T}}$

AND $\lambda_z = \frac{V \sin \alpha_v}{\Omega R}\sqrt{\frac{2 - 3\mu_v^2}{C_T}}$ - Concluded

λ_z	λ_x								
	2.40	2.80	3.20	3.60	4.00	5.00	6.00	8.00	10.00
2.40	0.315	0.285	0.261	0.239	0.210	0.184	0.156	0.120	0.097
2.20	.329	.295	.267	.245	.224	.186	.158	.121	.098
2.00	.344	.305	.275	.250	.228	.188	.159	.122	.099
1.80	.357	.315	.282	.256	.233	.191	.161	.122	.099
1.60	.370	.325	.289	.260	.237	.192	.162	.123	.099
1.40	.384	.333	.295	.265	.240	.195	.163	.124	.099
1.20	.395	.341	.301	.269	.243	.196	.164	.124	.099
1.00	.404	.347	.306	.272	.246	.197	.165	.124	.100
.80	.413	.352	.309	.276	.248	.198	.166	.125	.100
.60	.415	.356	.311	.277	.249	.199	.166	.125	.100
.40	.416	.357	.312	.278	.250	.200	.167	.125	.100
.20	.414	.357	.312	.278	.250	.200	.167	.125	.100
0	.410	.354	.310	.278	.250	.200	.167	.125	.100
-.20	.404	.350	.309	.275	.248	.199	.166	.125	.100
-.40	.395	.345	.305	.273	.247	.198	.166	.125	.100
-.60	.386	.339	.301	.270	.245	.197	.165	.125	.100
-.80	.374	.331	.296	.267	.242	.196	.165	.125	.100
-1.00	.362	.323	.290	.262	.239	.194	.164	.124	.099
-1.20	.349	.314	.284	.258	.235	.192	.163	.124	.099
-1.40	.337	.305	.277	.252	.231	.190	.161	.123	.099
-1.60	.325	.296	.270	.247	.227	.188	.160	.122	.099
-1.80	.312	.286	.263	.242	.223	.186	.158	.121	.098
-2.00	.300	.277	.255	.236	.219	.183	.157	.121	.098
-2.40	.278	.259	.241	.224	.209	.178	.153	.119	.097
-2.80	.258	.242	.227	.213	.200	.172	.149	.117	.096
-3.20	.239	.226	.214	.202	.191	.166	.145	.115	.095
-3.60	.222	.216	.201	.191	.182	.160	.141	.113	.094
-4.00	.207	.198	.189	.181	.173	.154	.137	.111	.093
-5.00	.175	.170	.164	.159	.155	.139	.127	.105	.089
-6.00	.152	.148	.144	.140	.137	.126	.117	.094	.085
-8.00	.118	.120	.115	.112	.111	.105	.093	.088	.078
-10.00	.096	.095	.094	.093	.092	.089	.085	.078	.070

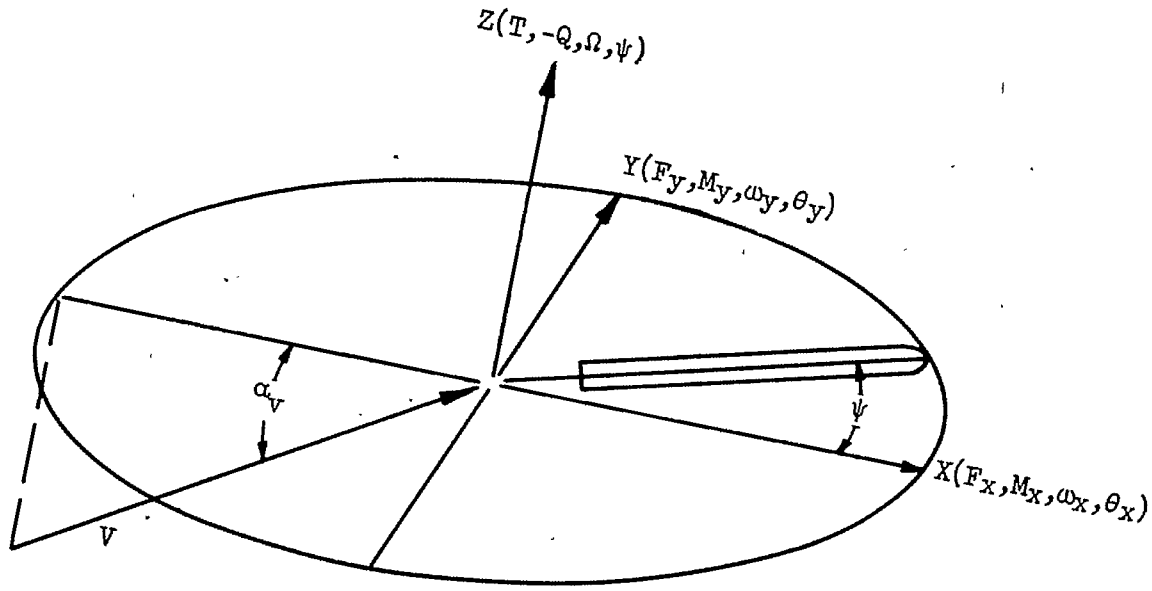

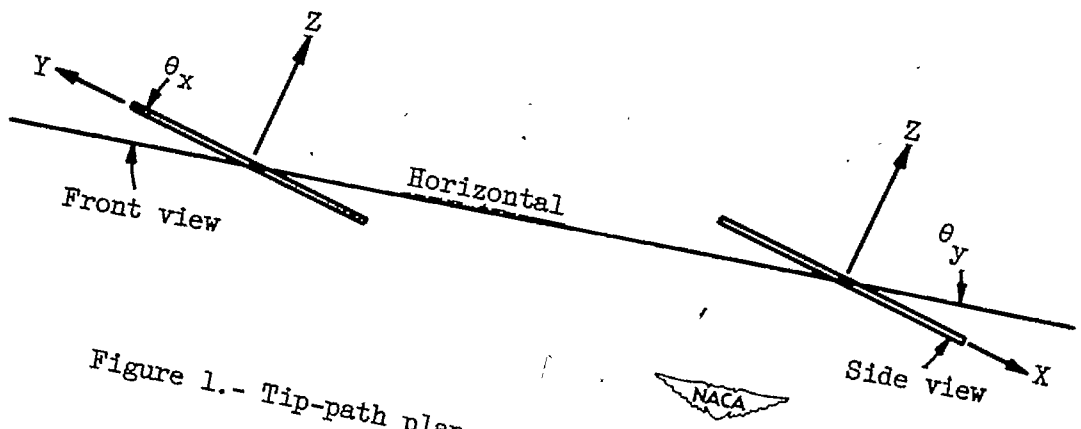

Figure 1.- Tip-path plane or axes of virtual rotation.

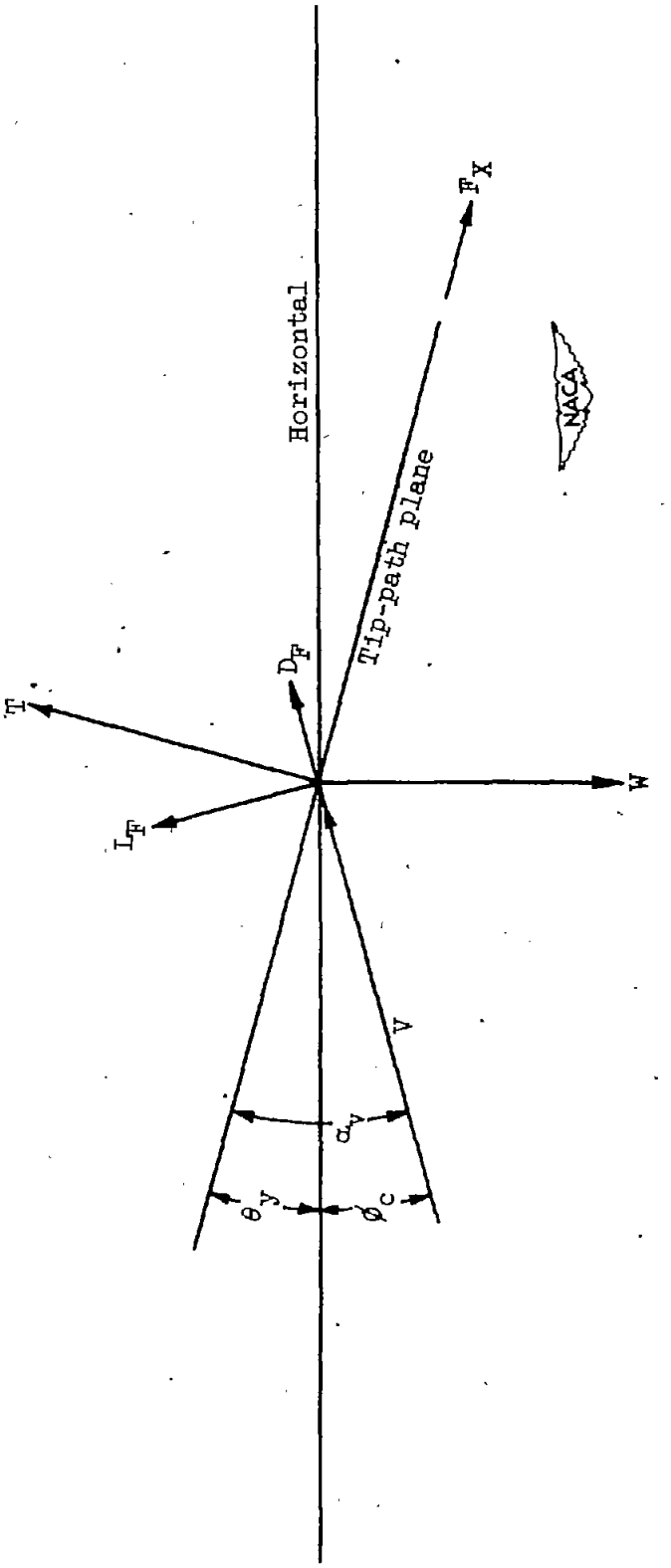

Figure 2.- Forces on rotor hub.

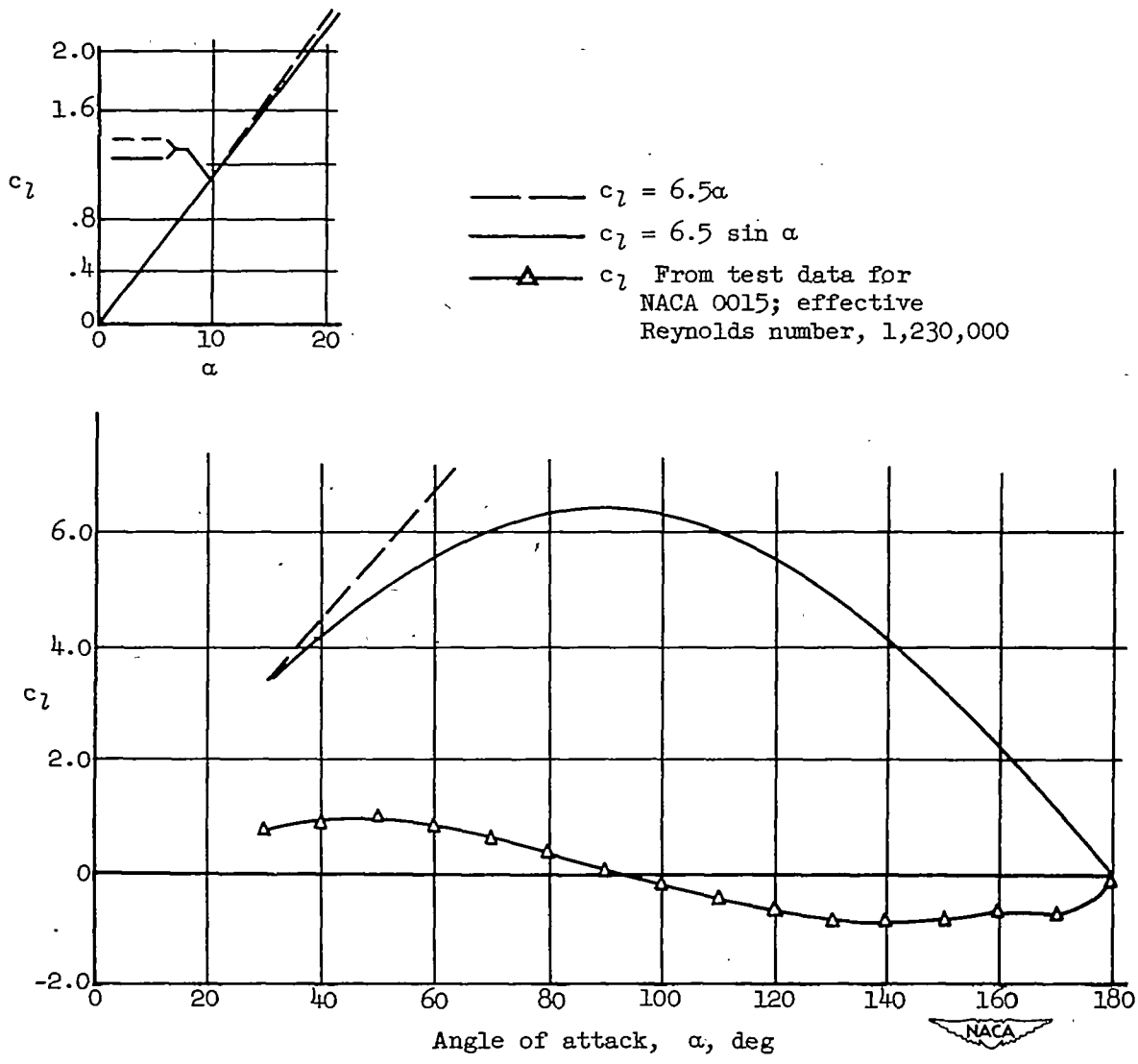

Figure 3.- Comparison of expressions for c_l.

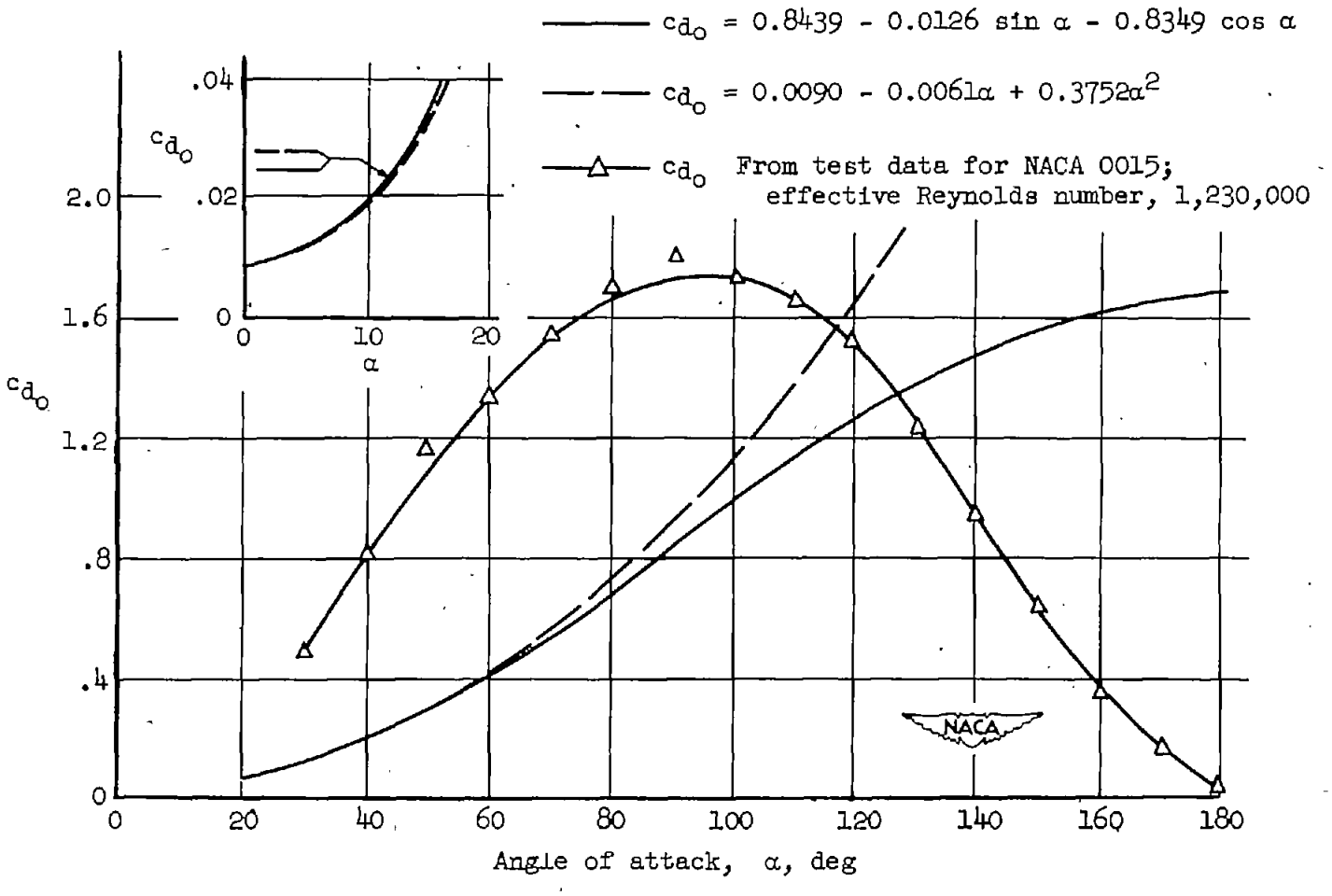

Figure 4.- Comparison of expressions for c_{d_o}.

NACA-Langley - 7-21-52 - 1000